Methods

Mice and reagents

Five-week-old female C57BL/6 mice were obtained from Charles River Japan (Yokohama, Japan). OT-I mice expressing $OVA_{257-264}$/H-2K^b–specific TCR were kindly provided by W. R. Heath (The Walter and Eliza Hall Institute, Melbourne, Australia) through H. Udono (RCAI, RIKEN, Yokohama, Japan). These mice were maintained under specific pathogen-free conditions, and used according to the guidelines of the institutional animal care and use committee established at Juntendo University and Tokyo Medical and Dental University. pcDNA3.1( ), pEF6/V5-TOPO, and pcDNA3.1-GFP-TOPO vectors were purchased from Invitrogen (Frederick, MD). PE-Mac1 (CD11b) mAb and control rat IgG2a were purchased from eBioscience (San Diego, CA). FITC-anti-CD11c mAb, PE-anti-V 2 mAb, and allophycocyanin (APC)–anti-CD8 mAb were purchased from BD Biosciences (San Jose, CA). Alexa Fluor 647–anti-CD8 mAb was purchased from Biolegend (San Diego, CA). 5-(and-6)-Carboxyfluorescein diacetate succinimidyl ester (CFSE) and 5-(and-6)-carboxytetramethylrhodamine succinimidyl ester (TAMRA) were purchased from Invitrogen. TdT and biotin-16-dUTP were purchased from Roche (Indianapolis, IN).

Generation of Tim-Igs and mAbs

The expression vectors for Tim-1–Ig, Tim-2–Ig, Tim-3–Ig, and Tim-4–Ig were generated by linking the extracellular domains of Tim-1 (aa 1-236), Tim-2 (aa 1-230), Tim-3 (aa 1-191), or Tim-4 (aa 1-288) to the Fc portion of mouse IgG2a in the pcDNA3.1( ) vector. Tim-Ig proteins were produced by transfection of each vector into HEK293T cells. The anti–mouse Tim-1 mAb (RMT1-17, rat IgG2a,), Tim-2 mAb (RMT2-14, rat IgG2a,), and Tim-3 mAb (RMT3-23, rat IgG2a,) were generated immunizing SD rats with Tim-1–Ig, Tim-2–Ig, and Tim-3–Ig, respectively, as described before.[23] Likewise, the anti–Tim-4 mAb (RMT4-54, rat IgG2a,) was generated by immunizing an SD rat with Tim-4–Ig, fusing lymph node cells with P3U1 myeloma cells, and screening the binding to CHO cells expressing Tim-4, but not parental CHO cells. For confocal microscopy, RMT3-23 was labeled with Alexa Fluor 594 using the mAb labeling kit (Invitrogen). Requests for mAbs should be addressed to H. Akiba (e-mail: hisaya@juntendo.ac.jp).

Cell lines

A normal rat kidney cell line (NRK-52E) was maintained in complete RPMI medium (RPMI 1640 supplemented with 10% FBS, 100 U/mL penicillin, 100 g/mL streptomycin, and 2 mM glutamine, 10 mM HEPES, and 50 M 2-mercaptoethanol). HEK293T cells (ATCC, Manassas, VA) were maintained in complete DMEM medium (DMEM supplemented with 10% FBS, 100 U/mL penicillin, 100 g/mL streptomycin, and 2 mM glutamine). For construction of expression vectors, the entire coding region of mouse Tim-1, Tim-2, Tim-3, or Tim-4 was subcloned into pMKITneo. Tim-3 cDNA was also subcloned into pEF6/V5-TOPO vector. Several mutant forms were prepared by polymerase chain reaction (PCR)–based mutagenesis using Tim-3/pEF6V5-TOPO as a template. After confirmation of nucleotide sequences, Tim expression vectors were transduced into NRK cells by electroporation with a Gene Pulser (Bio-Rad Laboratories, Hercules, CA). After selection with 1 mg/mL G418, cell surface expression was estimated by respective anti-Tim mAbs. HEK293T cells were transiently transfected with these expression vectors using lipofectAMINE2000 (Invitrogen). Two days after the transfection, cell surface expression of Tim was estimated by flow cytometry.

Phagocytosis assay

For preparation of apoptotic cells, thymocytes from C57BL/6 mice were labeled with 1 M CFSE or 10 g/mL TAMRA, and then were UV irradiated (100 J/cm^2). After UV irradiation, the cells were cultured in complete RPMI for 2 hours at 37°C, and then used for the phagocytosis assay. NRK cells (10^5 per well), NIH3T3 cells (5 10^4 cells per well), and HEK293T cells (10^5 cells per well) were plated onto 24-well plates, which were precoated with poly-L-lysine for HEK293T cells, a day before the phagocytosis assay. These cell lines were incubated with fluorescently labeled apoptotic cells (2 10^6 per well) at 37°C for the indicated periods. The recognition (binding and/or incorporation) of fluorescently labeled apoptotic cells by these cell lines was analyzed by flow cytometry using a FACSCalibur (BD Biosciences) and/or fluorescence microscopy using an Olympus FV1000 laser scanning confocal microscope (Melville, NY) equipped with 40 or 100 objective lens. For macrophages, peritoneal cells were harvested from C57BL/6 mice 3 days after intraperitoneal injection of 2 mL 3% wt/vol thioglycolate, or from untreated mice. These peritoneal cells (5 10^5 per well) were plated onto 48-well plate for 2 hours at 37°C, and then washed with PBS twice to remove floating cells. In some assay, macrophages were preincubated with the indicated mAb (30 g/mL) for 60 minutes at 4°C, and then washed with PBS to remove unbound mAb. Macrophages were cultured with fluorescently labeled apoptotic cells (2.5 10^6 per well) for 30 minutes at 37°C, and then washed with PBS 3 times to remove unbound apoptotic cells. After trypsinization, cells were harvested and stained with PE-Mac1. CFSE fluorescence intensity in Mac1 cells was analyzed on a FACSCalibur (BD Biosciences). As for an in vivo phagocytosis by PEM, sterile peritonitis was induced in C57BL/6 mice by intraperitoneal injection of 3% thioglycolate medium (2 mL per mouse). Three days later, these mice (n 4-5 per group) were treated intraperitoneally with control rat IgG (rIgG), RMT3-23, or RMT4-54 (200 g/mouse). Three hours later, mice were intraperitoneally injected with CFSE-labeled apoptotic cells (10^8 per mouse), and another 2 hours later, peritoneal cells were harvested. The recognition of apoptotic cells by Mac1 cells was analyzed by flow cytometry. For statistic evaluation, the unpaired Student *t* test, 2-tailed was used. *P* values less than .05 were considered significant. For in vitro phagocytosis assay using splenic DCs, spleens were digested with 400 U/mL collagenase (Wako Biochemicals) in the presence of 5 mM EDTA and separated into low- and high-density fractions on Optiprep gradient (Axis-Shield, Oslo, Norway). Low-density cells were purified using anti-CD11c MACS beads (Miltenyi Biotec, Auburn, CA). After staining CD11c cells with APC-anti-CD8 mAb, these cells (5 10^5 per well) were cocultured with TAMRA-labeled apoptotic cells (2.5 10^6 per well) in 48-well plate for the indicated periods, and then the cells were stained with FITC–anti-CD11c mAb. TAMRA fluorescence intensity in CD8 CD11c and CD8 CD11c cells was analyzed on a FACSCalibur. As for in vivo phagocytosis by splenic DCs, mice (n 3 per group) were treated intravenously with rIgG, or RMT3-23 and/or RMT4-54 (200 g each/mouse), and then 2 hours later, with CFSE-labeled apoptotic splenocytes (2 10^7 per mouse). Mice were killed at the indicated time points, and the recognition of apoptotic cells by CD8 CD11c cells was analyzed by flow cytometry. For statistic evaluation, the unpaired Student *t* test, 2-tailed was used. *P* values less than .05 were considered significant.

In situ identification of nuclear DNA fragmentation

C57BL/mice (n 4-6 per group) were treated intraperitoneally with rIgG, or RMT3-23 and/or RMT4-54 (200 g each per mouse) twice a week for 4 weeks. Three days after the final injection, mice were killed. Serum was stocked for measurement of anti-dsDNA antibody levels. Brain, liver, spleen, and pancreas were immersion-fixed in 20% buffered formalin and embedded in paraffin. After being deparaffinized, tissue sections were stained using in situ TUNEL method with biotin-16-dUTP (Roche Diagnostics, Basel, Switzerland) and diaminobenzidine as a peroxidase substrate. Nuclei were counterstained with hematoxylin. The number of TUNEL-positive cells was quantified with KS400 Image Analysis System (KS400; Zeiss, Heidelberg, Germany).

Measurement of anti-dsDNA antibody levels in serum

Serum levels of anti-dsDNA IgG were determined as described previously.[26] In brief, enzyme-linked immunosorbent assay (ELISA) plates were coated with 5 g/mL dsDNA derived from calf thymus (Sigma-Aldrich, St Louis, MO). Anti-dsDNA antibody level was expressed in units, referring to

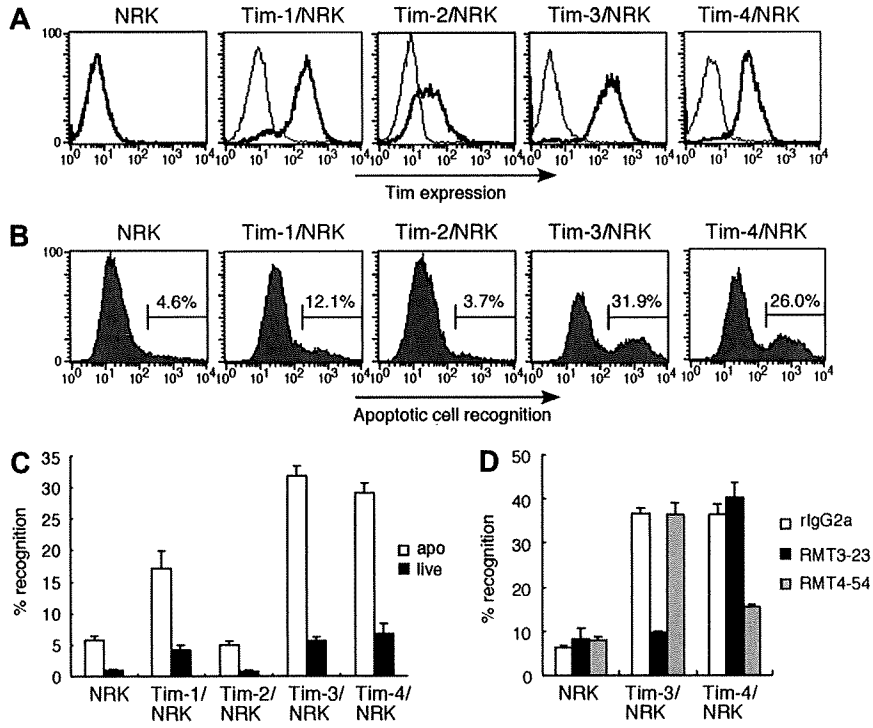

Figure 1. Tim-3 recognizes apoptotic cells. (A) NRK cells stably expressing Tim-1, Tim-2, Tim-3, or Tim-4 were stained with biotinylated anti–Tim-1 mAb (RMT1-17), anti–Tim-2 mAb (RMT2-14), anti–Tim-3 mAb (RMT3-23), or anti–Tim-4 mAb (RMT4-54), respectively. Parental NRK cells were stained with a cocktail of all mAbs. Then cells were stained with PE-avidin, and analyzed by flow cytometry (thick histogram). Thin histograms indicate background staining with control rat IgG2a, followed by PE-avidin. (B) These NRK cells were cultured with CFSE-labeled apoptotic cells for 30 minutes at 37°C. Recognition of apoptotic cells by these NRK cells was quantified by flow cytometry. (C) These NRK cells were cultured with CFSE-labeled viable cells or apoptotic cells for 30 minutes at 37°C. Percentage of the recognition was quantified by flow cytometry. Data are represented as mean SD of triplicates. (D) These NRK cells were pretreated with 20 g/mL control rIgG2a, RMT3-23, or RMT4-54 mAb, and then cultured with CFSE-labeled apoptotic cells for 30 minutes at 37°C. Percentage of the recognition was quantified by flow cytometry. Data are represented as mean SD of triplicates. Similar results were obtained in 3 (A-C) or 2 (D) independent experiments.

standard curve obtained by serial dilution of a standard serum pool from (NZB NZW) F1 mice older than 8 months, containing 1000 U activities/mL (kindly provided by S. Hirose, Juntendo University).

Flow cytometric analysis for Tim expression

Mouse macrophages or low-density splenocytes were pretreated with anti-FcR mAb (2.4G2), and then were incubated with 0.5 g biotinylated mAb for 30 minutes at 4°C, followed by PE-streptavidin and FITC-anti-CD11b mAb (for macrophages) or PE-streptavidin, FITC–anti-CD11c mAb and APC–anti-CD8 mAb (for splenic DCs). After washing with PBS, Tim expression on CD11b , CD8 CD11c , or CD8 CD11c cells was analyzed on a FACSCalibur, and the data were analyzed using the CellQuest program (BD Biosciences).

In vitro cross-presentation assay

OVA-loaded dying cells were prepared by osmotic shock as described previously.[12] For splenic DC subsets, CD11c cells purified using anti-CD11c MACS beads (92% CD11c) were then stained with FITC–anti-CD11c and APC–anti-CD8 mAbs, followed by sorting into subsets (89% CD8 CD11c ; 98% CD8 CD11c) on FACSVantage (BD Biosciences). OVA-loaded (10 mg/mL) dying cells (2.5 10^6 per well) were cocultured with CD8 DCs or CD8 DCs (5 10^5 per well) in presence of rIgG, RMT3-23, or RMT4-54 (30 g/mL) on 48-well plate for 1.5 hours, and then DCs were sorted again using anti-CD11c MACS beads. CD8 or CD8 DCs (both 10^4 or 2 10^3 per well) were cocultured with purified OT-I CD8 T cells (10^5 per well) in 96-well flat-bottom plate. For the direct presentation, CD8 or CD8 DCs (10^4 per well) were cocultured with 1 nM $OVA_{257-264}$ SIINFEKL peptides (AnaSpec, San Jose, CA) and OT-I CD8 T cells (10^5 per well) in presence of rIgG, RMT3-23, or RMT4-54 (30 g/mL) in 96-well flat-bottom plate. Two days later, 50 L supernatant was harvested and tested for IFN- production by sandwich ELISA (eBioscience). The cultures were then pulsed overnight with [^{3}H]thymidine (0.5 Ci [0.0185 MBq]/well; GE Healthcare, Little Chalfont, United Kingdom) and the uptake was measured in a microbeta counter (Microbeta Plus; Wallac, Turku, Finland).

In vivo cross-presentation assay

In vivo cross-presentation assay was performed as described previously[27] with minor modifications. CFSE-labeled OT-I cells (2 10^6 per mouse) were transferred intravenously into B6 mice. Next day, mice were injected intravenously with rIgG, or RMT3-23 and/or RMT4-54 (200 g each per mouse), and then 2 hours later, with OVA-loaded (1 mg/mL) dying splenocytes (10^7 per mouse). Two days later, mice were killed, and splenocytes were stained with PE–anti-V 2 and APC–anti-CD8. CFSE fluorescence intensity of CD8 V 2 cells was analyzed by flow cytometry.

Results

Tim-3 recognizes apoptotic cells and is recruited to phagosome

Because Tim-4 and Tim-1 are recently reported to recognize apoptotic cells,[8,9] we first verified the binding activity of NRK cells stably expressing Tim family molecules (Figure 1A) to apoptotic cells. As for apoptotic cells, we used UV (100 J/cm^2)–irradiated thymocytes because these cells show typical apoptotic phenotypes, which are annexin V and propidium iodide negative (PI) (Figure S1A, available on the *Blood* website; see the Supplemental Materials link at the top of the online article), and do not express Tim molecules (Figure S1B), excluding Tim-Tim interaction in this study. In addition to Tim-4/NRK and Tim-1/NRK, we found that Tim-3/NRK also efficiently bound apoptotic cells, but not live cells (Figure 1B,C), and that the binding of Tim-3/NRK and Tim-4/NRK cells to apoptotic cells was abrogated by anti–Tim-3 mAb RMT3-23 and anti–Tim-4 mAb RMT4-54, respectively (Figure 1D). These results suggest that Tim-3 as well as Tim-4 acts as a receptor for apoptotic cells.

To further address whether expression of Tim-3 could confer the ability to internalize or just bind apoptotic cells, we next used HEK293T cell reconstitution system because although ectopic expression of an authentic phagocytic receptor Fc RIII with FcR chain enabled this cell line to internalize IgG-opsonized bacteria, the expression of scavenger receptor-A (SR-A)[28] or paired Ig-like receptor-B (PIR-B),[29] which is the nonphagocytic receptor for bacteria, conferred the binding without significant internalization (not shown). As shown in

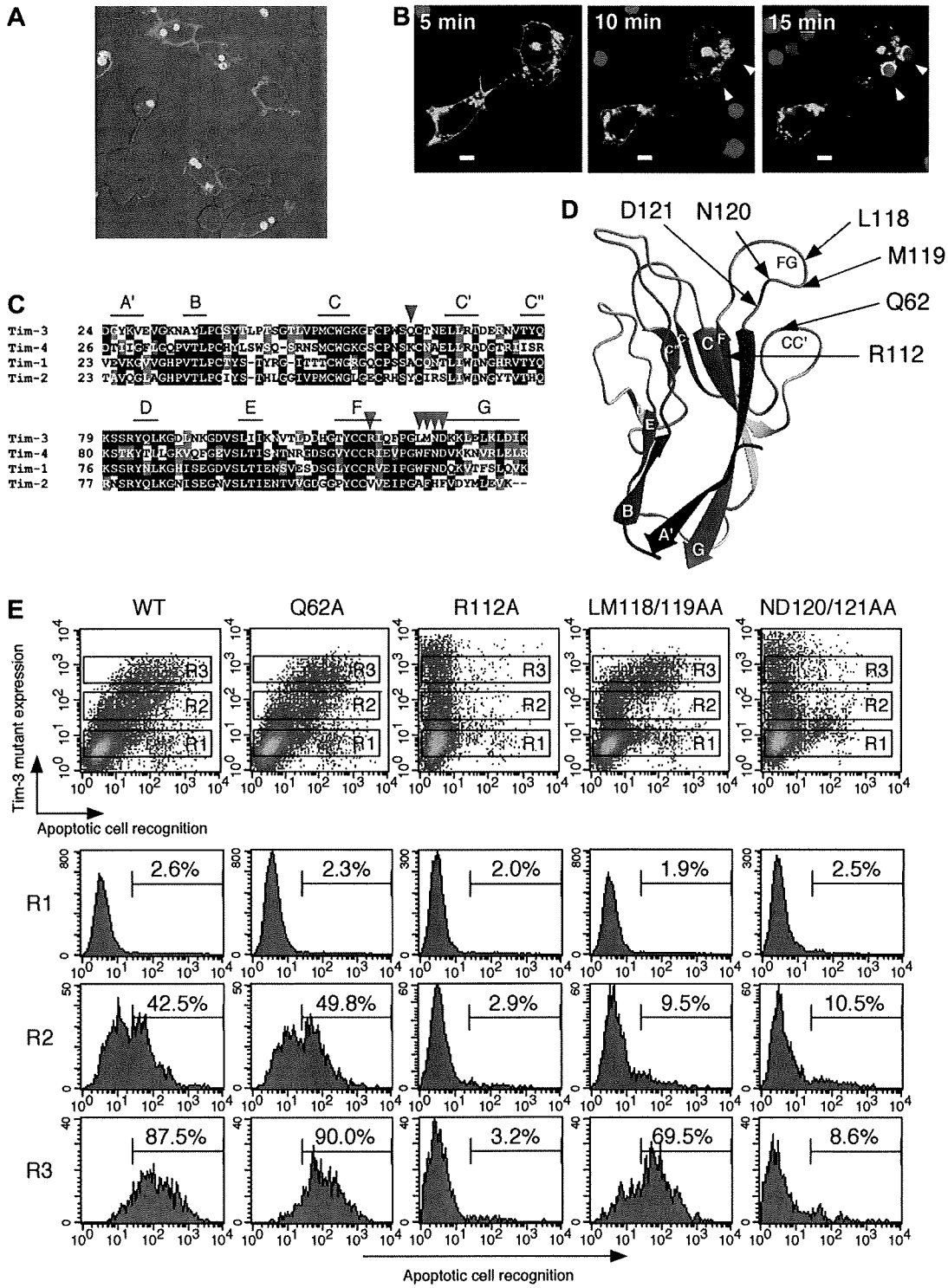

Figure 2. Tim-3 internalizes apoptotic cells through the FG loop in IgV domain. (A) HEK293T cells transiently expressing Tim-3 were cultured with CFSE-labeled apoptotic cells for 60 minutes at 37°C, and then cells were stained with biotinylated RMT3-23 and Alexa 594–avidin. (B) TAMRA-labeled apoptotic cells were added to HEK293T cells transiently expressing Tim-3-GFP under fluorescence microscope. Phagocytosis and Tim-3-GFP localization were analyzed at the indicated time points. White arrowheads indicate apoptotic cells internalized via Tim-3. White bars indicate 5 m. (C) Alignment of IgV domain of Tim family molecules. The -strands of Tim-3 were shown with lines. Mutated residues were indicated by red arrowheads. (D) Positions of mutated residues are indicated on 3-dimensional structure of Tim-3 IgV domain. The color of the protein main-chain is gradually changed along the sequence from blue (N-terminal) to red (C-terminal). (E) HEK293T cells transiently expressing wild-type or mutant Tim-3 were cultured with CFSE-labeled apoptotic cells for 60 minutes at 37°C, and then cells were stained with biotinylated RMT3-23 and PE-avidin. Recognition of apoptotic cells by gated HEK293T cells (R1; Tim-3 , R2; Tim-3^{low}, R3; Tim-3^{high}) was analyzed by flow cytometry. Similar results were obtained in 2 (A,B) or 3 (E) independent experiments.

Figure 2A, Tim-3–positive cells efficiently internalized CFSE-labeled apoptotic cells, indicating that Tim-3 is a phagocytic receptor for apoptotic cells. Furthermore, we addressed Tim-3 localization upon initial contact with apoptotic cells. To visualize Tim-3, we generated an expression vector for Tim-3 fused at its C-terminus to green fluorescence protein (GFP), and then expressed this fusion receptor in HEK293T cells. Whereas Tim-3 was mostly expressed at the cell surface in resting

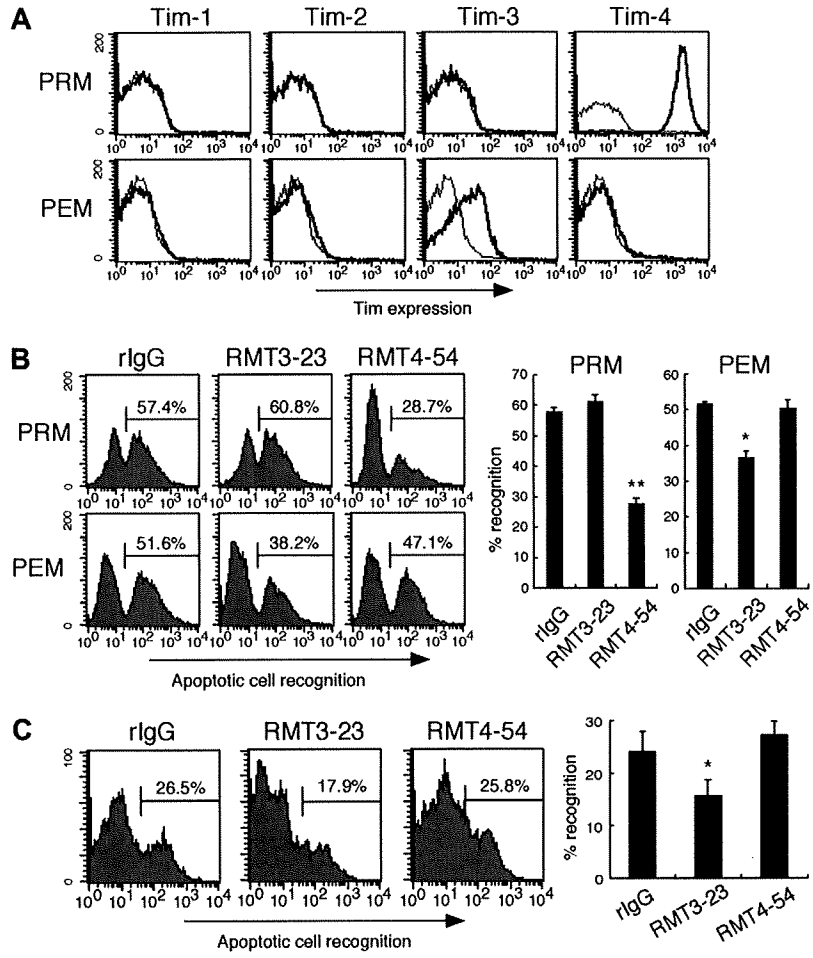

Figure 3. Tim-3 mediates phagocytosis of apoptotic cells by peritoneal exudate macrophages. (A) Peritoneal resident Mac1 cells (PRMs) and peritoneal exudate Mac1 cells (PEMs) were stained with biotinylated RMT1-17, RMT2-14, RMT3-23, or RMT4-54, followed by FITC-anti-CD11b mAb and PE-avidin (thick histograms); then CD11b cells were analyzed by flow cytometry. Thin histograms indicate background staining with biotinylated control rat IgG2a. (B) Macrophages were pretreated with control rat IgG2a (rIgG), RMT3-23, or RMT4-54, and then cultured with CFSE-labeled apoptotic cells for 30 minutes at 37°C. Cells were stained with PE-Mac1, and percentage of recognition of CFSE-apoptotic cells by Mac1 cells was quantified by flow cytometry. Columns represent mean SD of triplicates (*P .05; **P .01 compared with rIgG). (C) Peritonitis was elicited by intraperitoneal injection of thioglycolate. Three days later, the mice were intraperitoneally injected with rIgG, RMT3-23, or RMT4-54 (200 g/head), and then with CFSE-labeled apoptotic cells. Two hours later, peritoneal cells were harvested, and recognition of CFSE-labeled apoptotic cells by Mac1 cells was quantified by flow cytometry. The experiments (n 4-5 per group) were performed 3 times independently with a similar result. Columns represent mean SD of 4 mice in a representative experiment (*P .05 compared with rIgG). Similar results were obtained in 3 (A,C) or 2 (B) independent experiments.

conditions, upon recognition of TAMRA-labeled apoptotic cells, Tim-3 was recruited to the phagocytic cup (Figure 2B). This substantiates that Tim-3 mediates engulfment of apoptotic cells.

Tim-3 binds to PS

We next addressed whether Tim-3 also binds to phosphatidylserine (PS), a major "eat-me" signal,[1,2] by solid-phase ELISA using soluble Ig fusion proteins with extracellular domains including both IgV and mucin domains of Tim-2, Tim-3, and Tim-4. In addition to the strong binding of Tim-4-Ig to PS, we observed that Tim-3–Ig weakly but substantially bound to PS, but not other phospholipids such as phosphatidylethanolamine (PE), phosphatidylinositol (PI), and phosphatidylcholine (PC) (Figure S2A). Tim-2–Ig did not bind any phospholipids even at a high dose. The Tim-3–Ig or Tim-4–Ig binding to PS was abrogated by RMT3-23 or RMT4-54, respectively, in a dose-dependent manner (Figure S2B). These results indicate that Tim-3 recognizes PS, although the affinity is lower than that of Tim-4.

Tim-3 recognizes apoptotic cells through the FG loop in IgV domain

We next explored the Tim-3 recognition site of apoptotic cells. Recently, Santiago et al have revealed a crystal structure of Tim-4 and demonstrated that Tim-4 binds PS through the metal ion–dependent ligand binding site (MILIBS) in the FG loop, which is conserved in all Tim family members except Tim-2.[30] Thus, we specifically mutated some of amino acids locating around the FG loop of Tim-3 to alanine, and transiently transfected HEK293T cells with each mutant construct to address the relationship between expression level of each mutant and their phagocytic activities. We first replaced Gln62 or Arg112 to Ala because these amino acids, which locate in FG-CC cleft in the 3D structural model of Tim-3 IgV domain (Figure 2C,D), are critical for galectin-9–independent ligand binding.[31] Substitution of Gln62 did not alter the phagocytic activity, although substitution of Arg112 completely abrogated the activity (Figure 2E). We next addressed the putative MILIBS, which locates on the FG surface loop (Figure 2D). The LM118/119AA mutant recognized apoptotic cells only at high expression level, suggesting that substitution of these residues to both Ala weakened the activity (Figure 2E). The ND120/121AA mutant completely lost the activity (Figure 2E). These results suggest that Tim-3 internalizes apoptotic cells through the FG loop in IgV domain, and that at least in part galectin-9–independent ligand binding[31] might be linked to recognition of apoptotic cells.

Tim-3 and Tim-4 mediate phagocytosis of apoptotic cells by distinct macrophage subsets

We next examined the cell surface expression of Tim molecules on mouse primary macrophages, and their contribution to the phagocytosis of apoptotic cells. We found Tim-3 expression on peritoneal exudate Mac1 cells (PEMs), but not peritoneal resident Mac1 cells (PRMs) from naive mice (Figure 3A). In contrast, Tim-4 was highly expressed on PRMs, but not PEMs, which is consistent with

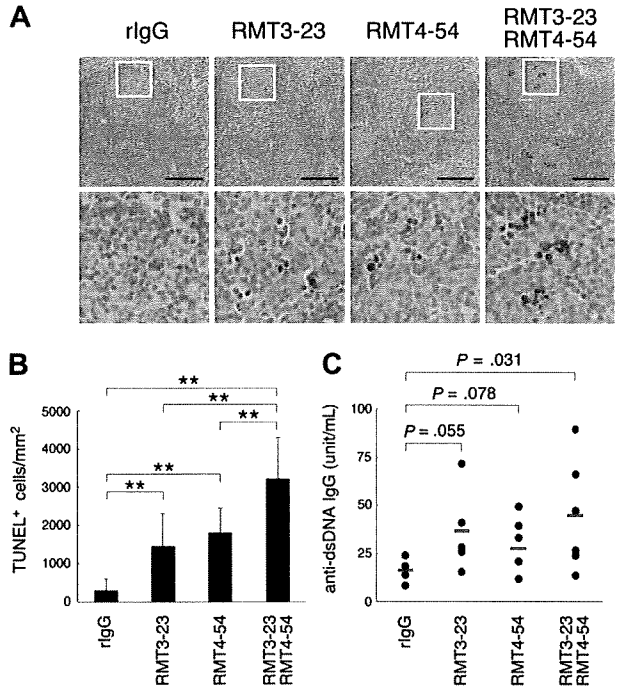

Figure 4. Involvement of Tim-3 in clearance of apoptotic cells in vivo. Mice (n 4-6 per group) were treated with rIgG, RMT3-23, and/or RMT4-54 (200 g each per mouse) twice a week for 4 weeks. (A) Apoptotic cells in paraffin-embedded spleen sections from these mice were detected by TdT-mediated dUTP nick-end labeling (TUNEL) method. Nuclei were counterstained with hematoxylin. Representative sections (top panels, 20 magnification) were shown. Black bars indicate 100 m. White squares mark the areas shown at a higher magnification (bottom panels, 80). (B) The number of TUNEL-positive cells was counted in at least 10 randomly chosen follicles, represented as columns (**P .01). (C) Anti-dsDNA antibody levels in serum were determined by ELISA. P values compared with rIgG are shown. Similar results were obtained in 2 independent experiments.

a previous report.[8] Neither Tim-1 nor Tim-2 was expressed on both types of macrophages (Figure 3A). This result prompted us to investigate whether these different types of macrophages use different Tim molecules to recognize apoptotic cells. As shown in Figure 3B, PRMs efficiently phagocytosed apoptotic cells, and this was significantly inhibited by RMT4-54, but not by RMT3-23. In contrast, phagocytosis of apoptotic cells by PEMs was significantly inhibited by RMT3-23, but not RMT4-54. These results suggest that although these macrophage subsets use MerTK and MFG-E8 to recognize and internalize apoptotic cells,[5,6,32] Tim-3 and Tim-4 also play a role in this process by PEMs and PRMs, respectively. Moreover, we used a mouse sterile peritonitis model to examine whether Tim-3 participates in the phagocytosis in vivo. As shown in Figure 3C, RMT3-23, but not RMT4-54, significantly inhibited the phagocytosis of apoptotic cells by peritoneal macrophages, suggesting that Tim-3 contributes to the phagocytosis of apoptotic cells in vivo.

Tim-3 is crucial for clearance of apoptotic cells in vivo

To evaluate the physiological role of Tim-3 and Tim-4 in vivo, we intraperitoneally injected RMT3-23 and/or RMT4-54 into C57BL/6 mice twice a week for 4 weeks, and stained apoptotic cells in various organs by terminal deoxynucleotidyl transferase–mediated deoxyuridine triphosphate nick-end labeling (TUNEL) method. In spleen follicles, treatment with either RMT3-23 or RMT4-54 significantly increased TUNEL cells, and a remarkable increase was observed with the combination treatment (Figure 4A,B), whereas the administration of these mAbs did not increase the number of TUNEL cells in the liver, pancreas, or brain (not shown).

It has been reported that an impairment of clearance of apoptotic cells induces autoantibody production.[5,33,34] Thus, we next measured serum level of autoantibodies in these mice. Consistent with a recent report,[8] blocking of Tim-4 by RMT4-54 induced anti-dsDNA antibodies (Figure 4C). We found that serum level of anti-dsDNA antibodies was also increased by RMT3-23 (Figure 4C). These results suggest that Tim-3 as well as Tim-4 participates in the clearance of apoptotic cells in vivo, and that the disabling of this system leads to autoantibody production.

Tim-3 mediates phagocytosis of apoptotic cells and cross-presentation by CD8 DCs in vitro

Because Tim-3 is involved in the clearance of apoptotic cells in not only inflammatory state (Figure 3C) but also steady state (Figure 4) in vivo, we further addressed the Tim-3 expression on several types of naive cells, and found that Tim-3 was highly expressed on peripheral blood monocytes and splenic DCs (Figure S3). Moreover, we noticed that the expression of Tim-3 on splenic CD8 DCs was approximately 3-fold higher than that on CD8 DCs (Figure 5A,B). Several groups have demonstrated that, in mouse spleen, CD8 DCs are uniquely able to recognize apoptotic cells, however, the receptor for apoptotic cells remains to be identified.[16-18] These reports prompted us to address whether Tim-3 plays a role for the recognition of apoptotic cells by this DC subset. Consistent with previous reports,[16,35] we observed that CD8 DCs recognized apoptotic cells more efficiently than CD8 DCs (Figure 5C). Interestingly, masking of Tim-3 by RMT3-23 inhibited approximately 50% recognition of apoptotic cells by CD8 DCs (Figure 5C,D), suggesting that CD8 DCs use Tim-3 to efficiently recognize apoptotic cells. Confocal microscopy revealed that, although Tim-3 is largely expressed at cell surface of naive CD8 DCs (Figure 5E left panel), upon recognition of apoptotic cells Tim-3 is recruited to the site of apoptotic cell apposition with the membrane (Figure 5E right panel), suggesting that Tim-3 mediates internalization of apoptotic cells by CD8 DCs.

Because CD8 DC is the splenic DC subset that plays a crucial role in cross-presentation,[15] we next performed cross-presentation study using OT-I T cells specific for $OVA_{257-264}$/H-2K^b. Consistent with previous reports,[15,16] we confirmed that CD8 DCs cultured with OVA-loaded, but not BSA-loaded, apoptotic cells could efficiently induce OT-I CD8 T-cell proliferation, and that OT-I cells did not directly respond to OVA-loaded apoptotic cells (Figure S4). Then, we investigated the requirement of Tim-3 for this cross-presentation. As shown in Figure 6A, we observed that CD8 DCs induced OT-I T-cell proliferation more vigorously than CD8 DCs, and that inhibition of the phagocytosis by RMT3-23 significantly abrogated the CD8 DC-induced OT-I cell proliferation. Moreover, we observed a remarkable reduction in IFN- production by RMT3-23 (Figure 6B), whereas both DC subsets loaded with $OVA_{257-264}$ peptides equally activated OT-I T cells, irrespective of masking Tim-3 by RMT3-23. Although splenic DCs express Tim-4 at low level, RMT4-54 did not inhibit the phagocytosis of apoptotic cells and the cross-presentation in vitro (Figures 5,6).

Tim-3 is crucial for phagocytosis of apoptotic cells and cross-presentation in vivo

We further addressed the contribution of Tim-3 to the phagocytosis of apoptotic cells and cross-presentation by CD8 DCs in vivo. It has been reported that intravenously injected apoptotic cells are taken up mainly by CD8 DCs in mouse spleen.[16,35] Consistently,

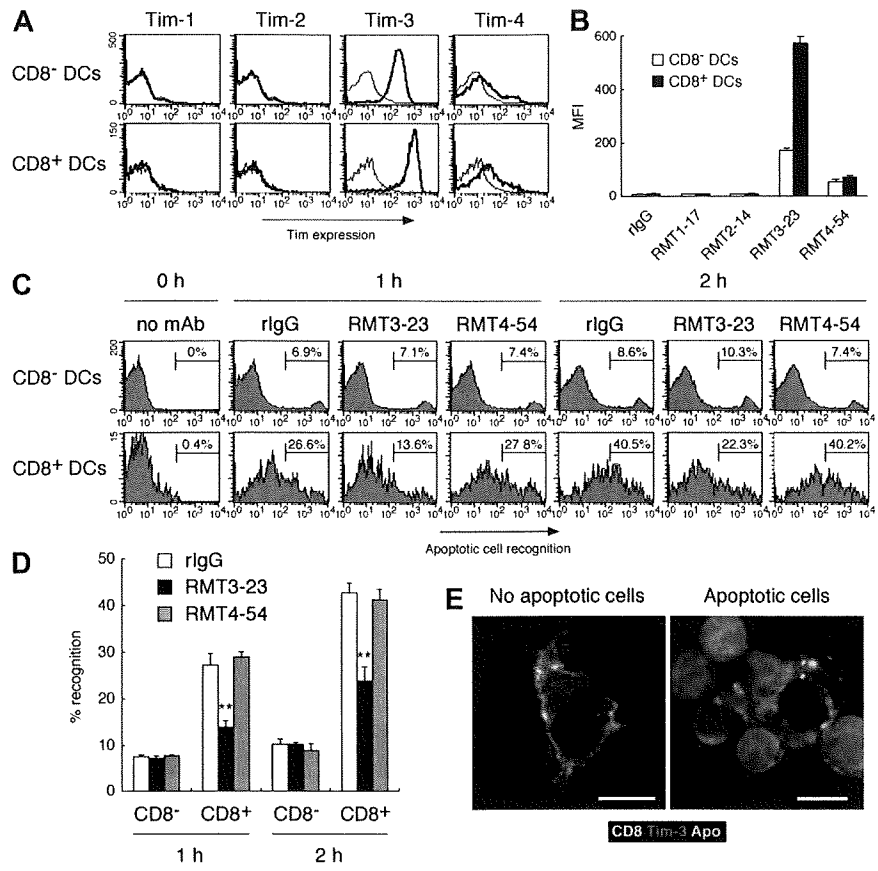

Figure 5. Tim-3 mediates phagocytosis of apoptotic cells by CD8 DCs. (A) Low-density splenocytes were stained with biotinylated control rIgG2a (thin histograms), RMT1-17, RMT2-14, RMT3-23, or RMT4-54 (thick histograms), followed by PE-avidin, FITC–anti-CD11c mAb, and APC–anti-CD8 mAb; then Tim expression on CD8 CD11c or CD8 CD11c cells was analyzed by flow cytometry. The average of mean fluorescence intensity (MFI) SD of triplicates is represented in panel B. (C) Purified splenic CD11c cells prestained with APC–anti-CD8 mAb were treated with rIgG, RMT3-23, or RMT4-54, and then cultured with TAMRA-labeled apoptotic cells at 37°C. After the indicated time period, cells were stained with FITC–anti-CD11c mAb, and percentage recognition of TAMRA-labeled apoptotic cells by CD8 CD11c or CD8 CD11c cells was quantified by flow cytometry. Columns represent mean SD of triplicates in panel D (**P .01 compared with rIgG). (E) (Left panel) Purified splenic CD11c cells were stained with Alexa 647–anti-CD8 mAb and Alexa 594–RMT3-23. (Right panel) Purified splenic CD11c cells prestained with Alexa 647–anti-CD8 mAb were cultured with CFSE-labeled apoptotic cells for 60 minutes at 37°C, and then cells were stained with Alexa 594–RMT3-23. Cells were analyzed by confocal microscopy. White bars indicate 5 m. Similar results were obtained in 3 (A-D) or 2 (E) independent experiments.

we also observed that CD8 DCs efficiently recognized CFSE-labeled apoptotic cells 1 hour after intravenous injection (Figure 7A,B). Interestingly, the recognition was significantly abrogated by RMT3-23. To rule out the possibility that binding of RMT3-23 to FcR on DCs might affect phagocytosis of apoptotic cells, we pretreated mice with anti-FcR (2.4G2). As shown in Figure S5C, 2.4G2 did not affect the blocking activity of RMT3-23. Moreover, we prepared F(ab)$_2$ fragments of RMT3-23, and observed that the F(ab)$_2$ fragments did not lose the blocking effect (Figure S5), indicating that the blocking effect of RMT3-23 is not mediated through FcRs. These results suggest that Tim-3 is crucial for the recognition of apoptotic cells by CD8 DCs in vivo.

To study cross-presentation of apoptotic cell–associated antigens in vivo, we transferred CFSE-labeled OT-I T cells into C57BL/6 mice, and then 1 day later, we primed these mice with OVA-loaded dying splenocytes. Two days after the priming, we observed that OT-I cells proliferated vigorously in spleen (Figure 7C,D), although OT-I cells did not proliferate in unprimed mouse spleen, indicating that dying cell-associated OVA antigens were taken up by splenic CD8 DCs and cross-presented to OT-I cells. Consistent with a crucial role of Tim-3 for the uptake of apoptotic cells by CD8 DCs (Figure 7A,B), the proliferation of OT-I cells was also significantly reduced by RMT3-23, but not RMT4-54 (Figure 7C,D). These results suggest that Tim-3 plays a crucial role in phagocytosis of apoptotic cells and subsequent cross-presentation by CD8 DCs in vivo.

Discussion

Phagocytes such as macrophages and DCs efficiently recognize and engulf apoptotic cells to maintain the peripheral tolerance. In this study, we demonstrate that Tim-3 mediates phagocytosis of apoptotic cells by PEMs and CD8 DCs, and that disabling of the Tim-3 function in vivo induces autoantibody production. Likewise, several studies have shown that impairment of the clearance of apoptotic cells causes autoantibody production,[5,8,34] however, the mechanism for the elicited immune response to dying cells remains to be elucidated. As the possible explanation, delay or impairment of clearance of apoptotic cells by macrophages causes secondary necrotic cells releasing intracellular contents, which could be endogenous "danger signal" activating immune system.[1] However, chronic administration of apoptotic thymocytes to syngeneic mice induces more remarkable level of autoantibody production than that of the same dose of nonapoptotic cell lysate,[36] suggesting that autoantibody production in response to dying cells could not be explained simply by the exposure of the intracellular contents. It has also been reported that, in mice, CD8 DC subset is unique in its ability to recognize apoptotic cells and cross-present dying cell-associated antigens.[15,16] It is considered that, in steady state, cross-presentation of dying cell-associated self-antigens by CD8 DCs induces autoreactive CD8 T-cell proliferation abortively, subsequently resulting in their deletion, which is important to maintain peripheral tolerance.[10,13,14] Taken together, Tim-3–mediated phagocytosis of apoptotic cells by CD8 DCs may be linked to peripheral tolerance, and a loss of Tim-3 function in DCs may exacerbate autoimmunity. Consistent with this hypothesis, we and others have reported that Tim-3 negatively regulates Th1-mediated inflammatory diseases such as EAE, type I diabetes, and aGVHD, and promotes tolerance induction.[21-23]

Alternatively, however, upon being activated by anti-CD40 mAb, endogenous danger signals such as heat shock proteins and uric acid, or pathogen-associated molecular patterns (PAMPs) such as LPS and CpG, DCs turn to cross-prime CD8 T cells to generate

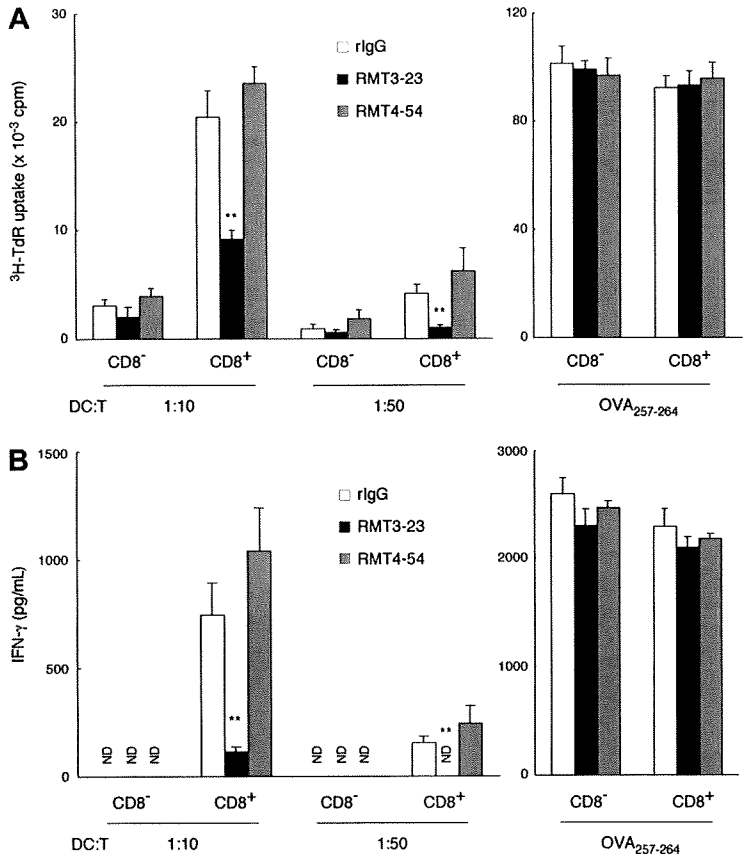

Figure 6. Tim-3–mediated phagocytosis of apoptotic cells is crucial for the cross-presentation by CD8 DCs. (A) Purified CD8 CD11c or CD8 CD11c splenic DCs were pretreated with rIgG (white histograms), RMT3-23 (black histograms), or RMT4-54 (gray histograms) and then cultured with OVA-loaded apoptotic cells. After 2 hours, both DC subsets were purified again to remove dead cells, and then cocultured with OT-I CD8 T cells at the indicated ratio. For the direct presentation, both DC subsets preincubated with $OVA_{257-264}$ peptide (1 nM) in the presence of rIgG, RMT3-23, or RMT4-54 were cocultured with OT-I CD8 T cells at a 1:10 (DC/T) ratio. [^{3}H]thymidine (^{3}H-TdR) uptake was measured at 48 to 60 hours. (B) Production of IFN- in the culture supernatant at 48 hours after addition of OT-I CD8 T cells was measured by ELISA. Columns represent mean SD of triplicates (**P .01 compared with rIgG). ND indicates not detectable. Similar results were obtained in 3 independent experiments (A,B).

effector cells.[10,12] Given that Tim-3 is crucial for IFN- production in cross-presentation and that Tim-3 is expressed on sterile inflammatory macrophages, Tim-3 may promote induction of effector CD8 T-cell proliferation and functional memory under pathological conditions. Indeed, Anderson et al have recently reported that Tim-3 expressed on DCs exacerbates a Th1-type autoimmune disease EAE.[25] Although Tim-3 has been reported to have multiple functions,[21-23] it would be important to further address whether this novel function of Tim-3 is linked to immune tolerance or activation under pathological conditions.

It remains unclear why CD8 DCs are not able to engulf apoptotic cells efficiently, although this DC subset expresses Tim-3. One possibility is that the phagocytic activity may be determined by relative expression level of receptors for "eat-me" signals and "don't eat-me" signals. Although we observed that expression level of Tim-3 on CD8 DCs is approximately 3-fold higher than that on CD8 DCs, it has been reported that signal-regulatory protein (SIRP) , a receptor for "don't eat-me" signal,[37] is much more highly expressed on CD8 DCs than CD8 DCs.[38] Taken together, a high expression of Tim-3 may be required for the phagocytosis by DCs, and/or SIRP may neutralize Tim-3 function on CD8 DCs. Moreover, phagocytic activity of each cell type may be determined not only by expression level of the phagocytic receptor, but also cell-intrinsic phagocytic machinery such as cytoskeletal architecture. Indeed, Tim-3 as well as Tim-1 is expressed on activated T cells,[24,39] but these T cells are not able to recognize apoptotic cells.

In this study, ectopic expression of Tim-3 enabled HEK293T cells to engulf whole apoptotic cells. However, Miyanishi et al could not observe the phagocytic activity of Tim-3 expressed on NIH3T3 cells based on their engulfment assay, which quantified nuclear DNA degradation of apoptotic cells engulfed by NIH3T3 expressing Tim-3 and DNase II.[8] To address this discrepancy, we also generated NIH3T3 cells expressing Tim-3, and did not observe the ability of Tim-3 to mediate engulfment of whole apoptotic cells, although we did observe the ability of Tim-3 to incorporate CFSE-labeled apoptotic cell debris (Figure S6). The reason why Tim-3 expressed on NIH3T3 cells is not able to efficiently phagocytose apoptotic cells remains to be elucidated. We cannot rule out the possibility that Tim-3 may recognize apoptotic cells in cooperation with some coreceptor, which may be expressed on HEK293T cells, macrophages, and CD8 DCs, but not NIH3T3 cells or CD8 DCs. Likewise, it has been reported that although gene targeting of MerTK receptor results in remarkable defect of phagocytosis of apoptotic cells by macrophages,[5] the receptor requires coexpression of $_V$ $_5$ integrin to enable NIH3T3 cells to recognize apoptotic cells.[40] Although we did observe PS binding of Tim-3 by solid-phase ELISA, Miyanishi et al failed to observe this by PIP–strip binding assay.[8] This discrepancy is probably due to a difference in assay sensitivity. Given that the affinity of Tim-3 to PS is much lower than that of Tim-4, Tim-3 might bind not only PS but also some other ligand to phagocytose apoptotic cells. Further studies are needed to elucidate the complexity of phagocytosis.

We show here a crucial role of Tim-3 for clearance of apoptotic cells in vivo and differential expression profile of phagocytic Tim molecules, suggesting that the pathophysiological roles of each Tim molecule appear to be different. Because Tim-1 is expressed on epithelial cells but not professional phagocytes, Tim-1 may contribute to remodeling of injured epithelia.[9] Tim-4 is highly expressed on PRMs, and contributes to the phagocytosis of apoptotic cells during physiological tissue turnover.[8] Our findings highlight Tim-3 as the phagocytic receptor responsible for cross-presentation by CD8 DCs. This novel function of Tim-3 opens the door to new therapeutic approaches to combat infections, cancers, and autoimmune diseases.

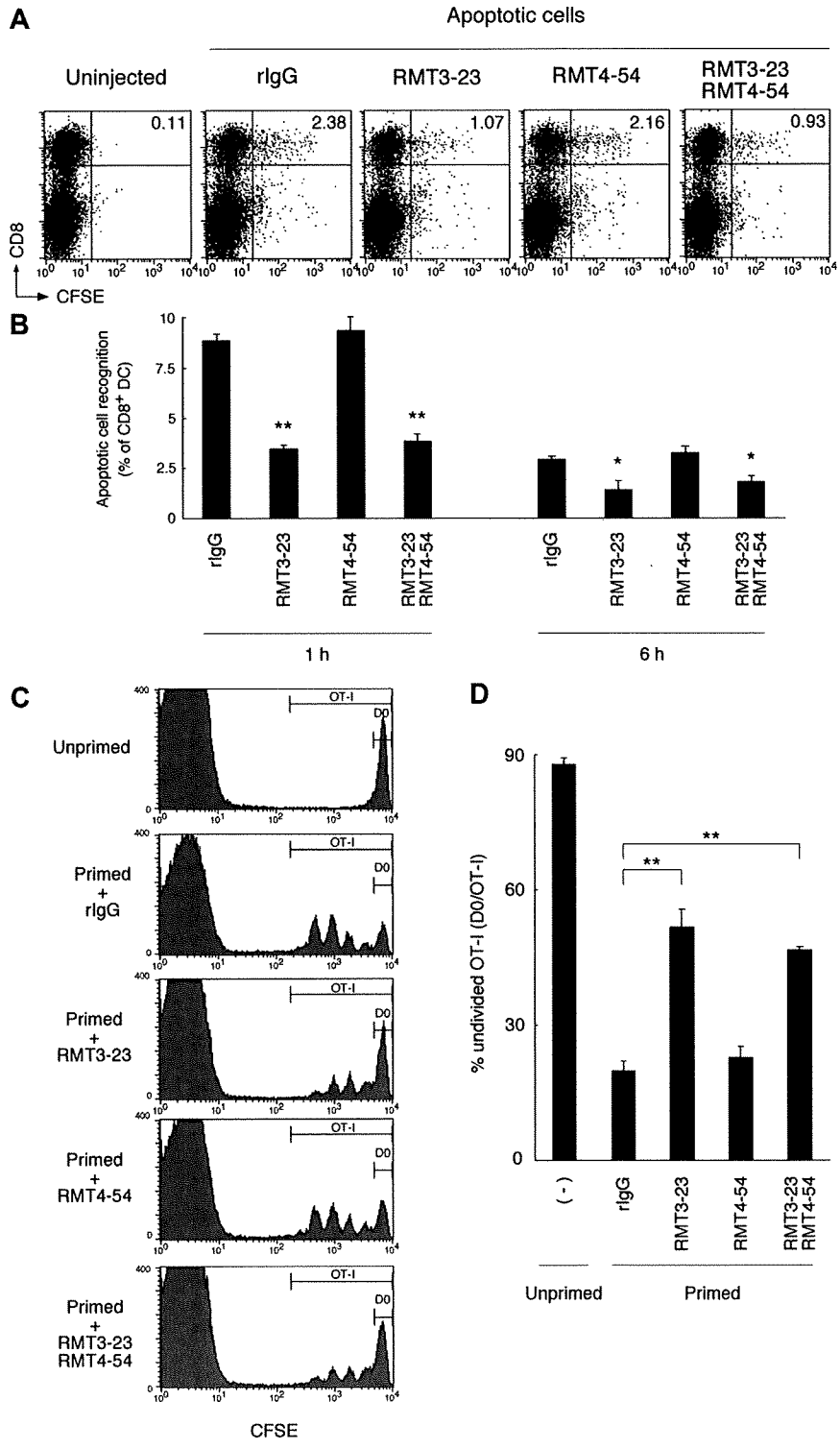

Figure 7. Tim-3 is crucial for the phagocytosis of apoptotic cells and cross-presentation in vivo. (A) Mice (n 3 per group) were intravenously injected with the indicated mAb (200 g each per head), and then 2 hours later with CFSE-labeled apoptotic splenocytes (2 10^7 per head). One hour later, collagenase-digested splenocytes were harvested, and recognition of CFSE-labeled apoptotic cells by splenic CD11c cells was analyzed by flow cytometry. Numbers indicate percentage of cells in top right quadrants. (B) Collagenase-digested splenocytes were harvested from mice treated as described in panel A at indicated time points, and recognition of apoptotic cells by splenic CD8 DCs was analyzed by flow cytometry. Percentage recognition of CFSE-labeled apoptotic cells by CD8 DCs (percentage CFSE CD8 CD11c cells/percentage CD8 CD11c cells 100) was calculated. Columns represent mean SD of triplicates (*P .05; **P .01 compared with rIgG). Similar results were obtained in 3 independent experiments. (C) CFSE-labeled OT-I CD8 T cells (2 10^6 per head) were intravenously transferred into B6 mice (n 3 per group). The next day, mice were intravenously injected with the indicated mAb (200 g each per head), and then 2 hours later primed with OVA-loaded apoptotic cells (10^7 per head). Two days later, whole splenocytes were harvested, and CFSE intensity of CD8 V 2 OT-I cells was analyzed by flow cytometry. Percentage of undivided cells in total OT-I cells (D0 per OT-I in C) was calculated, and mean SD of triplicates was shown in panel D (**P .01 compared with rIgG). Similar results were obtained in 3 independent experiments.

Acknowledgments

We thank Drs William R. Heath for OT-I mice, Sachiko Hirose for aged (NZB NZW) F1 mice serum, and Toshio Kitamura for pMXs-IRES-puro vector. We also thank Dr Tamami Sakanishi for cell sorting.

This work was supported by the Grants-in-Aid for Scientific Research from the Japanese Ministry of Education, Culture, Sports, Science and Technology (Tokyo, Japan), and by a grant from "High-Tech Research Center" Project for Private Universities: matching fund subsidy from the Ministry of Education, Culture, Sports, Science and Technology (Tokyo, Japan).

Authorship

Contribution: M.N. designed and performed experiments; H.A. provided vital reagents; H.A., Y.K., and M.H. discussed experimental strategy and performed experiments; K.T. designed and discussed experimental strategy; M.A., H.Y., and K.O. supervised

experiments and discussed the experimental strategy; M.N. wrote the paper; and K.T. and H.Y. edited the paper.

Conflict-of-interest disclosure: The authors declare no competing financial interests.

Correspondence: Masafumi Nakayama, Department of Immunology, Juntendo University School of Medicine, 2-1-1 Hongo, Bunkyo-ku, Tokyo 113-8421, Japan; e-mail: nakayama@juntendo.ac.jp.

References

1. Savill J, Dransfield I, Gregory C, Haslett C. A blast from the past: clearance of apoptotic cells regulates immune responses. Nat Rev Immunol. 2002;2:965-975.
2. Henson PM, Hume DA. Apoptotic cell removal in development and tissue homeostasis. Trends Immunol. 2006;27:244-250.
3. Cohen JJ, Duke RC, Fadok VA, Sellins KS. Apoptosis and programmed cell death in immunity. Annu Rev Immunol. 1992;10:267-293.
4. Ravichandran KS, Lorenz U. Engulfment of apoptotic cells: signals for a good meal. Nat Rev Immunol. 2007;7:964-974.
5. Scott RS, McMahon EJ, Pop SM, et al. Phagocytosis and clearance of apoptotic cells is mediated by MER. Nature. 2001;411:207-211.
6. Hanayama R, Tanaka M, Miwa K, Shinohara A, Iwamatsu A, Nagata S. Identification of a factor that links apoptotic cells to phagocytes. Nature. 2002;417:182-187.
7. Park D, Tosello-Trampont AC, Elliott MR, et al. BAI1 is an engulfment receptor for apoptotic cells upstream of the ELMO/Dock180/Rac module. Nature. 2007;450:430-434.
8. Miyanishi M, Tada K, Koike M, Uchiyama Y, Kitamura T, Nagata S. Identification of Tim4 as a phosphatidylserine receptor. Nature. 2007;450:435-439.
9. Kobayashi N, Karisola P, Pena-Cruz V, et al. TIM-1 and TIM-4 glycoproteins bind phosphatidylserine and mediate uptake of apoptotic cells. Immunity. 2007;27:927-940.
10. Heath WR, Belz GT, Behrens GM, et al. Cross-presentation, dendritic cell subsets, and the generation of immunity to cellular antigens. Immunol Rev. 2004;199:9-26.
11. Kurts C, Kosaka H, Carbone FR, Miller JF, Heath WR. Class I-restricted cross-presentation of exogenous self-antigens leads to deletion of autoreactive CD8( ) T cells. J Exp Med. 1997;186:239-245.
12. Liu K, Iyoda T, Saternus M, Kimura Y, Inaba K, Steinman RM. Immune tolerance after delivery of dying cells to dendritic cells in situ. J Exp Med. 2002;196:1091-1097.
13. Redmond WL, Sherman LA. Peripheral tolerance of CD8 T lymphocytes. Immunity. 2005;22:275-284.
14. Luckashenak N, Schroeder S, Endt K, et al. Constitutive crosspresentation of tissue antigens by dendritic cells controls CD8 T cell tolerance in vivo. Immunity. 2008;28:521-532.
15. den Haan JM, Lehar SM, Bevan MJ. CD8( ) but not CD8( ) dendritic cells cross-prime cytotoxic T cells in vivo. J Exp Med. 2000;192:1685-1696.
16. Iyoda T, Shimoyama S, Liu K, et al. The CD8 dendritic cell subset selectively endocytoses dying cells in culture and in vivo. J Exp Med. 2002;195:1289-1302.
17. Schulz O, Pennington DJ, Hodivala-Dilke K, Febbraio M, Reis e Sousa C. CD36 or alphavbeta3 and alphavbeta5 integrins are not essential for MHC class I cross-presentation of cell-associated antigen by CD8 alpha murine dendritic cells. J Immunol. 2002;168:6057-6065.
18. Belz GT, Vremec D, Febbraio M, et al. CD36 is differentially expressed by CD8 splenic dendritic cells but is not required for cross-presentation in vivo. J Immunol. 2002;168:6066-6070.
19. Monney L, Sabatos CA, Gaglia JL, et al. Th1-specific cell surface protein Tim-3 regulates macrophage activation and severity of an autoimmune disease. Nature. 2002;415:536-541.
20. Anderson AC, Anderson DE. TIM-3 in autoimmunity. Curr Opin Immunol. 2006;18:665-669.
21. Sabatos CA, Chakravarti S, Cha E, et al. Interaction of Tim-3 and Tim-3 ligand regulates T helper type 1 responses and induction of peripheral tolerance. Nat Immunol. 2003;4:1102-1110.
22. Sánchez-Fueyo A, Tian J, Picarella D, et al. Tim-3 inhibits T helper type 1-mediated auto- and alloimmune responses and promotes immunological tolerance. Nat Immunol. 2003;4:1093-1101.
23. Oikawa T, Kamimura Y, Akiba H, et al. Preferential involvement of Tim-3 in the regulation of hepatic CD8 T cells in murine acute graft-versus-host disease. J Immunol. 2006;177:4281-4287.
24. Zhu C, Anderson AC, Schubart A, et al. The Tim-3 ligand galectin-9 negatively regulates T helper type 1 immunity. Nat Immunol. 2005;6:1245-1252.
25. Anderson AC, Anderson DE, Bregoli L, et al. Promotion of tissue inflammation by the immune receptor Tim-3 expressed on innate immune cells. Science. 2007;318:1141-1143.
26. Xiu Y, Nakamura K, Abe M, et al. Transcriptional regulation of Fcgr2b gene by polymorphic promoter region and its contribution to humoral immune responses. J Immunol. 2002;169:4340-4346.
27. Li M, Davey GM, Sutherland RM, et al. Cell-associated ovalbumin is cross-presented much more efficiently than soluble ovalbumin in vivo. J Immunol. 2001;166:6099-6103.
28. Peiser L, Gough PJ, Kodama T, Gordon S. Macrophage class A scavenger receptor-mediated phagocytosis of Escherichia coli: role of cell heterogeneity, microbial strain, and culture conditions in vitro. Infect Immun. 2000;68:1953-1963.
29. Nakayama M, Underhill DM, Petersen TW, et al. Paired Ig-like receptors bind to bacteria and shape TLR-mediated cytokine production. J Immunol. 2007;178:4250-4259.
30. Santiago C, Ballesteros A, Martinez-Munoz L, et al. Structures of T cell immunoglobulin mucin protein 4 show a metal-Ion-dependent ligand binding site where phosphatidylserine binds. Immunity. 2007;27:941-951.
31. Cao E, Zang X, Ramagopal UA, et al. T cell immunoglobulin mucin-3 crystal structure reveals a galectin-9-independent ligand-binding surface. Immunity. 2007;26:311-321.
32. Hu B, Jennings JH, Sonstein J, et al. Resident murine alveolar and peritoneal macrophages differ in adhesion of apoptotic thymocytes. Am J Respir Cell Mol Biol. 2004;30:687-693.
33. Asano K, Miwa M, Miwa K, et al. Masking of phosphatidylserine inhibits apoptotic cell engulfment and induces autoantibody production in mice. J Exp Med. 2004;200:459-467.
34. Hanayama R, Tanaka M, Miyasaka K, et al. Autoimmune disease and impaired uptake of apoptotic cells in MFG-E8-deficient mice. Science. 2004;304:1147-1150.
35. Schnorrer P, Behrens GM, Wilson NS, et al. The dominant role of CD8 dendritic cells in cross-presentation is not dictated by antigen capture. Proc Natl Acad Sci U S A. 2006;103:10729-10734.
36. Mevorach D, Zhou JL, Song X, Elkon KB. Systemic exposure to irradiated apoptotic cells induces autoantibody production. J Exp Med. 1998;188:387-392.
37. Gardai SJ, McPhillips KA, Frasch SC, et al. Cell-surface calreticulin initiates clearance of viable or apoptotic cells through trans-activation of LRP on the phagocyte. Cell. 2005;123:321-334.
38. Lahoud MH, Proietto AI, Gartlan KH, et al. Signal regulatory protein molecules are differentially expressed by CD8- dendritic cells. J Immunol. 2006;177:372-382.
39. de Souza AJ, Oriss TB, O'Malley KJ, Ray A, Kane LP. T cell Ig and mucin 1 (TIM-1) is expressed on in vivo-activated T cells and provides a costimulatory signal for T cell activation. Proc Natl Acad Sci U S A. 2005;102:17113-17118.
40. Wu Y, Singh S, Georgescu MM, Birge RB. A role for Mer tyrosine kinase in alphavbeta5 integrin-mediated phagocytosis of apoptotic cells. J Cell Sci. 2005;118:539-553.

Exp. Anim. 58(2), 159–168, 2009

—Original—

T Cell Receptor Repertoire in BALB/c Mice Varies According to Tissue Type, Sex, Age, and Hydrocortisone Treatment

Kazutaka KITAURA[1–3], Kiichi KANAYAMA[4], Yoshiki FUJII[1,2], Noriyuki SHIOBARA[1], Konagi TANAKA[1], Ichiro KURANE[2], Satsuki SUZUKI[5], Tsunetoshi ITOH[6], and Ryuji SUZUKI[1]

[1]Department of Rheumatology and Clinical Immunology, Clinical Research Center for Allergy and Rheumatology, National Sagamihara Hospital, 18–1 Sakuradai, Sagamihara, Kanagawa 228-0815, [2]Department of Virology I, National Institute of Infectious Diseases, Tokyo 162-8640, [3]Department of Infection Biology, Institute of Basic Medical Sciences, University of Tsukuba, Ibaraki 305-8575, [4]Laboratory of Veterinary Physiology, Department of Veterinary Medicine, College of Bioresource Sciences, Nihon University, Fujisawa, Kanagawa 252-8510, [5]Section of Biological Science Research Center for Odontology, Nippon Dental University School of Dentistry at Tokyo, Chiyoda-ku, Tokyo 102-8159, and [6]Division of Immunology and Embryology, Department of Cell Biology, Tohoku University School of Medicine, Sendai 980-8574, Japan

Abstract: Diversity in T cell recognition of antigens is determined by diverse usage of T cell receptor (TCR) repertoire. TCR repertoire analysis provides fundamental information for understanding T cell immune responses in the pathogenesis of various diseases. In the present study, we examined the TCR repertoire in various tissues in normal BALB/c mice. The TCR α chain variable region repertoires were consistent among the spleen, lymph nodes, and the thymus. The TCR β chain variable region (TCRBV) repertoires were consistent between the spleen and lymph nodes, but different in the thymus. The TCR repertoires also differed in the lungs and the intestinal tract. The TCR repertoires were consistent between male and female mice, except for TCRBV15-1. TCR repertoire was almost similar in 3- and 7-week-old mice, except for TCRBV1-1, 8-3, and 14-1. The present findings suggest that the TCR repertoire of mice varies according to tissue type, sex and age. Additional analysis of the TCR repertoire, i.e., the effect of hydrocortisone (HC), was carried out. After the HC treatment, although the thymic T cells decreased to one-tenth, only a small fraction of $CD4^+CD8^+$ T cells survived the treatment. Furthermore, the percentages of thymic T cells bearing TCRBV3-1, 5-1, 5-2, and 16-1 substantially decreased, but the percentage of cells bearing TCRBV12-1 did not decrease. The present findings suggest that the HC susceptibility of immature thymic T cells is different between TCR families.

Key words: FACS, hydrocortisone, real-time PCR, repertoire, T cell receptor

(Received 26 September 2008 / Accepted 25 December 2008)

Address corresponding: R. Suzuki, Department of Rheumatology and Clinical Immunology, Clinical Research Center for Allergy and Rheumatology, National Sagamihara Hospital, 18–1 Sakuradai, Sagamihara, Kanagawa 228-0815, Japan

Introduction

Diversity in antigen recognition is established by TCR α and β gene rearrangements through several stages of differentiation and maturation in the thymus [7, 8, 12, 18]. In addition to rearrangements of the TCR α and β genes comprising variable (V), diversity (D), and joining (J) loci, random nucleotide insertions (N regions) occur in the D-J region, leading to the formation of enormously diverse TCR repertoire [4]. After completion of TCR gene rearrangement in the cortex of the thymus, T cells migrate to the medulla. Through positive and negative selection, only clones with moderate affinities for major histocompatibility complex (MHC) molecules are selected. The selected T cells then emigrate from the thymus to the peripheral lymphatic tissues. The peripheral T cells recognize peptide fragments presented by MHC molecules via their TCRs, subsequently becoming activated, and produce various cytokines and proliferate.

T cells play important roles in recovery from infectious diseases [6, 23] as well as in the pathogenesis of allergic and autoimmune diseases [1, 17, 22, 27]. Analysis of TCR repertoires provides important information for understanding immunopathological mechanisms. As a base for TCR repertoire analyses in diseases, it is necessary to determine the TCR repertoires in the tissues of healthy individuals.

The effects of HC administration on T cells in the thymus have been described. Although HC treatment causes massive deletion of immature thymocytes, the biological significance of the effect of HC on thymocyte differentiation still remains unsolved. The HC-resistant thymocyte population, considered to be equivalent to medullary thymocytes, has similar phenotypes and functions to those of mature T cells [3, 10, 11]. On the other hand, it is known that the thymic cortex $CD62^+$ T cell shows HC resistance [20]. Generally, the HC affects various responses *in vivo* such as blood pressure, glucose elevation, anti-inflammatory action, and immunosuppression. However, there is no detailed report of the TCR repertoire of the HC response in the thymus.

In the present study, we analyzed the relative expression levels of CD3, a T cell marker, and usage of TCR repertoires in various tissues in BALB/c mice. We also compared the TCR repertoires between male and female mice, and between 3-week-old (sexual immature group) and 7-week-old (sexual mature group) mice. Furthermore, we examined the TCR repertoire in BALB/c mice after HC administration, and compared the TCR repertoire of the thymus, with those of the peripheral lymphatic organ, the spleen. To analyze the TCR repertoires, we used adaptor-ligation-mediated PCR (AL-PCR) and microplate hybridization assay (MHA) methods [6, 13, 23, 28]. Generally, other previous methods of TCR analysis were using many TCRV specific probes in independent PCRs. However, precise quantification was difficult, because amplification efficiencies differ among individual primers. The AL-PCR ligates universal primer to the variable region 5' end of the TCR gene and is able to amplify all TCR genes in one PCR. Moreover, the MHA has V/C values which have coherent strict color development intensities for all TCR genes determined by the ratio of the hybridization intensity of each TCR variable region-specific probe to that of the corresponding TCR constant region-specific probe. The analysis of the relative abundances of the TCRs are related to the MHA, the mRNA of the TCR gene, and the FACS analysis using monoclonal antibodies for each TCR [28]. Therefore, TCR repertoire analysis using the AL-PCR and MHA methods enables us to amplify and measure all the variable regions of the rearranged TCR genes without any artificial skewing.

Materials and Methods

Animals

Specific pathogen free (SPF) BALB/cAnCrj ($H\text{-}2^d$) mice were purchased from Charles River Japan Inc. (Tokyo, Japan). The mice were housed under barrier conditions with a temperature of 23 ± 3°C, relative humidity of 55 ± 15%, and a 12-h light/dark cycle. Irradiated commercial laboratory mouse chow (CRF-1, ORIENTAL YEAST Co, Ltd., Japan) and autoclaved water were provided *ad libitum*. Animal experiments were performed according to the Guidelines of the Committee of Animal Experiments of Sagamihara National Hospital Clinical Research Center for Allergy and Rheumatology.

Study 1: Analysis of TCR repertoire in normal BALB/c mice

Five mice in one group (four groups: 3 and 7 weeks of age, males and females, total 20 mice) were sacrificed by exsanguination under isoflurane anesthesia, and their spleens, lymph nodes, thymuses, lungs, intestinal tracts, livers, genital organs (uteruses and seminal vesicles), bone marrows, and brains were collected. Total RNA samples were isolated from these tissues using an RNeasy Mini Kit (QIAGEN Sciences, Maryland, USA) according to the manufacturer's instructions.

Real-time PCR

The CD3 mRNA expression levels in the total RNA samples were examined by real-time PCR using a LightCycler apparatus (Roche Diagnostics, Basel, Switzerland). Total RNA (500 ng) was converted to cDNAs using a PrimeScript™ RT Reagent Kit (Takara Bio, Otsu, Japan) according to the manufacturer's instructions. PCR amplification was performed using SYBR® Premix Taq™ (Takara Bio) for SYBR® Green I. A primer pair specific for CD3 (forward primer: CACTCTGGGCTTGCTGATGG; reverse primer: TCATAGTCTGGGTTGGGAACAGG) was purchased from Takara Bio. Briefly, the PCR amplification was carried out in a 20-μl final volume containing 2 μl of DNA template, 0.4 μl of 10 μM solutions of the CD3 forward and reverse primers, 10 μl of SYBR® Premix Taq™ and H_2O up to 20 μl. After an initial denaturation step at 95°C for 10 s, 50 cycles of 95°C for 5 s and 60°C for 30 s were performed, with measurement of the fluorescence at the end of each cycle. Immediately after the amplification, a melting curve analysis was performed from 65°C to 95°C at a linear temperature transition rate of 0.1°C/s with continuous recording of fluorescence. The absolute copy numbers of unknown samples were calculated by comparing the threshold cycles with the corresponding standard curve. A reference cDNA was used in every assay to correct experimental variations among assays. The cDNA levels among samples were normalized by the expression level of the internal control gene glyceraldehyde-3-phosphate dehydrogenase (GAPDH) [25]. Quantification was based on the relative ratio between each unknown sample and the reference sample. To include all measurement mRNAs, the reference sample was mixed with total RNA of various organs and tissues.

AL-PCR

To analyze the TCR repertoires, samples were amplified by AL-PCR as previously described [13, 28]. Briefly, freshly isolated RNA (1 μg) was converted to double-stranded cDNAs using SuperScript™ II RNase H⁻ Reverse Transcriptase (Invitrogen, California, USA) according to the manufacturer's instructions, except that a specific primer (BSL-18E) was used. P10EA/P20EA adaptors were ligated to the 5' ends of the cDNAs and the adaptor-ligated cDNAs were cut with *SphI*. First and second PCR amplifications were performed with TCR α chain constant region (TCRAC)-specific or TCR β chain constant region (TCRBC)-specific primers and P20EA. A third PCR amplification was performed using both P20EA and 5'-biotinylated TCRAC- or TCRBC-specific primers for biotinylation of PCR products. All PCR amplifications were performed in triplicate.

MHAs

The TCR α chain variable region (TCRAV) and TCR β chain variable region (TCRBV) repertoires were analyzed by MHAs [13, 14, 28]. Briefly, 10 pmol of amino-modified oligonucleotides specific for TCRAV and TCRBV segments were immobilized in carboxylate-modified 96-well microplates (C type; Sumitomo Bakelite, Tokyo, Japan) with water-soluble carbodiimide. The probes used in the present study were described previously [28]. The names of the TCR families and probes were designed in order of the genomic TCR gene name, except for the pseudogene. Prehybridization and hybridization were performed in GM Church (GMC) buffer (pH 7.0) comprising 0.5 M Na_2HPO_4, 1 mM EDTA, 7% SDS and 1% BSA at 47°C. Denatured 5'-biotinylated PCR products (40 μl) were mixed with an equivalent volume of 0.4 N NaOH/10 mM EDTA, and added to 4 ml of GMC buffer. An aliquot (100 μl) of the hybridization solution was placed in each well of the microplate containing immobilized oligonucleotide probes specific for the V segment. After hybridization, the wells were washed six times with washing buffer (2 × SSC, 0.1% SDS) at room temperature. For stringent washing, the plate was incubated at 37°C for 10 min. After three washes, 200 μl of TB-TBS buffer (pH 7.4) comprising

10 mM Tris-HCl, 0.5 M NaCl, 0.5% Tween 20, and 0.5% blocking reagent (Roche Diagnostics, Mannheim, Germany) was added to block non-specific binding. Next, 100 μl of alkaline phosphatase-conjugated streptavidin (R&D Systems, Minnesota, USA) diluted 1:5000 in TB-TBS was added, and the plate was incubated at 37°C for 30 min. After six washes in T-TBS (10 mM Tris-HCl pH7.4, 0.5 M NaCl, 0.5% Tween 20), color development was initiated by adding 100 μl of substrate solution, 4 mg/ml p-nitrophenylphosphate (Nacalai Tesque, Kyoto, Japan), to 10% diethanolamine (pH 9.8). After 1 h, the absorbance was determined at 405 nm. Data were analyzed using the Ascent software package (Thermo Fisher Scientific, Massachusetts, USA). The V/C value was determined using TCR cDNA-concentrated samples containing the appropriate V segment and the universal C segment, respectively [28]. The absorbance obtained for each TCRV-specific probe was divided by the corresponding V/C value. The relative frequencies were calculated based on the corrected absorbance using the following formula: relative frequency (%) = [(corrected absorbance of TCRV-specific probe) / (sum of corrected absorbance of TCRV-specific probes)] × 100.

Study 2: Analysis of TCR repertoire in HC treated mice

The HC treatment of mice was performed by a modified Reichert *et al.* method [20]. In brief, a group of five 3-week-old male mice were administered i.p. with 5.0 mg of HC acetate (Wako, Osaka, Japan) dissolved in 200 μl of saline. A separate group of five mice were administered i.p. with 200 μl of saline and served as controls. At 48 h after the administration, all mice were sacrificed by exsanguination under isoflurane anesthesia, and their thymuses and spleens were collected. In these samples, flow cytometry analysis and TCR repertoire analysis (according to the method of total RNA isolation, AL-PCR and MHAs) were carried out.

Flow cytometry analysis

Cell suspensions were prepared in PBS containing 5% BSA (BSA-PBS). Thymus and spleen cells were stained with the following monoclonal antibodies: CyChrome-conjugated American Hamster anti-CD3ε (145-2C11; BD PharMingen, New Jersey, USA); fluorescein isothiocyanate (FITC)-conjugated rat anti-CD4 (H129.19; BD PharMingen); and phycoerythrin (PE)-conjugated rat anti-CD8a (53-6.7; BD PharMingen). After staining, cells were washed with BSA-PBS and analyzed on a FACS-Calibur flow cytometer (Becton Dickinson, California, USA) using the CellQuest software. Cells were gated on forward scatter/ side scatter plots and then on CD3.

Table 1. Comparison of CD3 mRNA expression levels in organs and tissues[a)]

Organs and tissues	Relative expression[b)] (%) ± SD
Spleen	75.8 ± 2.6
Lymph nodes	145.4 ± 8.6
Thymus	82.2 ± 8.5
Lungs	24.5 ± 1.2
Intestinal tract	4.6 ± 0.1
Liver	1.4 ± 0.1
Seminal vesicles	2.0 ± 0.1
Uterus	0.4 ± 0.1
Bone marrow	1.7 ± 0.1
Brain	0.1 ± 0.1

[a)]The assay was performed by five independent experiments. The assay results indicate the ratio of the number of T cells and/or expression intensity of T cell receptors in organs and tissues. [b)]The relative expression (%) represents the percentage value of each sample divided by the reference sample.

Statistical analysis

Differences between groups were analyzed by Student's paired *t*-test using StatView 5.0 for Windows (SAS Institute, North Carolina, USA). *P* values of <0.05 were accepted as statistically significant.

Results

Comparison of CD3 expression in various organs

The CD3 mRNA expression levels were analyzed in the spleen, lymph nodes, the thymus, the lung, the intestinal tract, the liver, the genital organs (uterus and seminal vesicles), the bone marrow, and the brain of normal 3-week-old male BALB/c mice (Table 1). The expression levels of CD3 in the spleen, lymph nodes and the thymus were notably greater than those in the lung and the intestinal tract. Whereas the liver, genital organs (the uterus and the seminal vesicle), the bone marrow, and the brain expressed extremely low levels of CD3 compared to the lung and the intestinal tract. Similar CD3 expression patterns were found in female mice (data not shown).

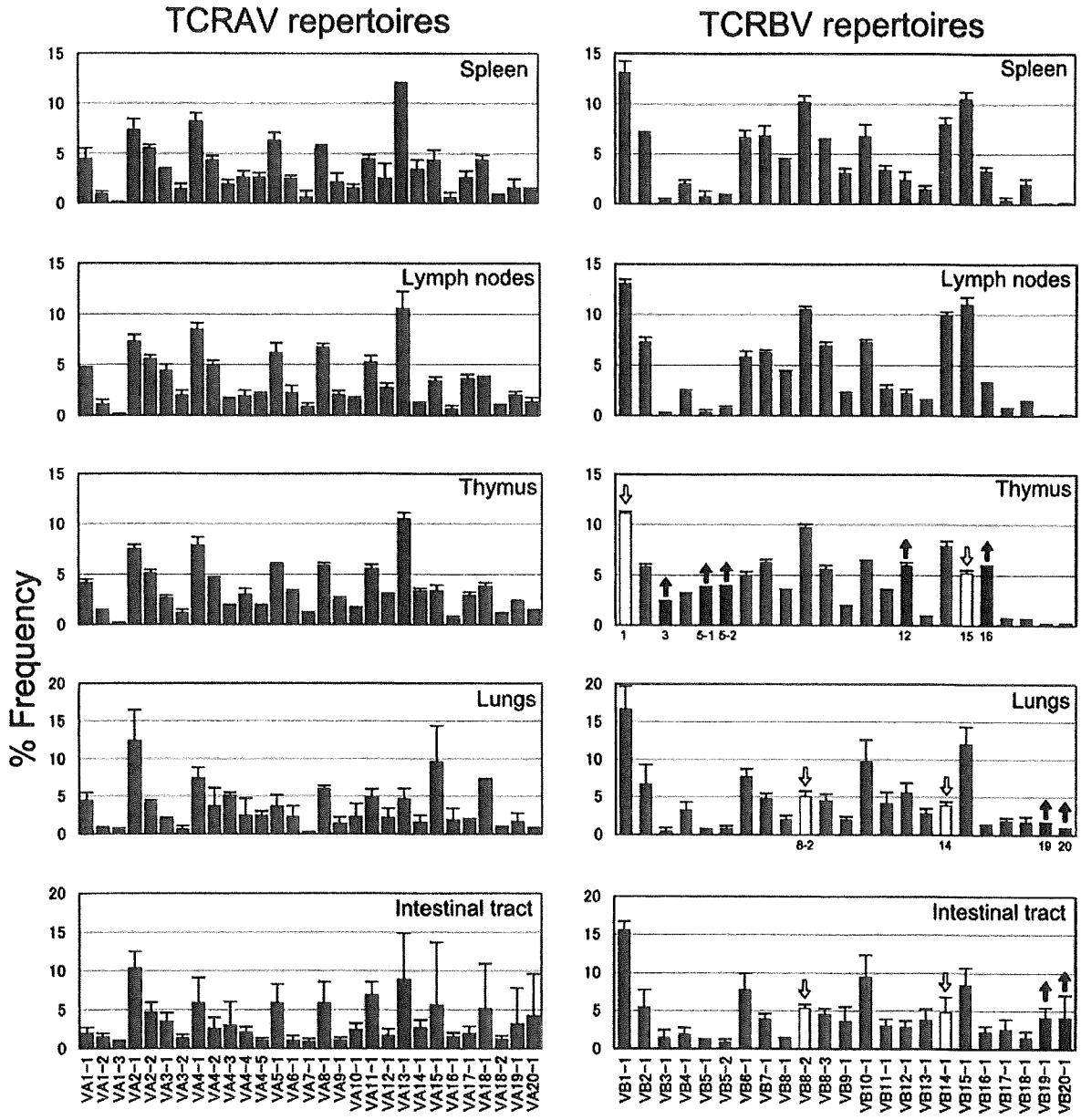

Fig. 1. TCRAV and TCRBV repertoires in tissues of 3-week-old male BALB/c mice. The percentages of cells bearing each TCR are shown for the spleen, lymph nodes, the thymus, the lung, and the intestinal tract. Vertical error bars indicate the standard deviation of five independent experiments. In the thymus, the percentages of cells bearing TCRBV3-1, 5-1, 5-2, 12-1, and 16-1 were significantly increased ($P<0.05$; black arrows and bars) and the percentages of cells bearing TCRBV1-1 and 15-1 were significantly decreased ($P<0.05$; white arrows and bars) compared with the corresponding levels in the spleen. In the lungs and the intestinal tract, percentages of cells bearing TCRBV19-1 and 20-1 were significantly increased ($P<0.05$; black arrows and bars) and the percentages of cells bearing TCRBV8-2 and 14-1 were significantly decreased ($P<0.05$; white arrows and bars) compared with the corresponding levels in the spleen.

Determination of TCRAV and TCRBV repertoires in tissues

The TCR repertoires of 3-week-old male BALB/c mice were analyzed in various organs and representative TCR repertoires are shown in Fig. 1. The TCRAV repertoires were consistent among the spleen, lymph nodes, and thymus, while the TCRBV repertoires were consistent between the spleen and lymph nodes. The TCRBV

repertoires in the thymus differed from those in the spleen and lymph nodes. In the thymus, the percentages of cells bearing TCRBV3-1, 5-1, 5-2, 12-1, and 16-1 were significantly increased and those of cells bearing TCRBV1-1 and 15-1 were significantly decreased in comparison with the spleen and lymph nodes.

The TCRAV and TCRBV repertoires in the lung and intestinal tract differed from those in the spleen, lymph nodes, and the thymus. Smaller numbers of TCRBV8-2- and TCRBV14-1-bearing cells were detected in the lung and the intestinal tract compared to the lymphatic organs. On the other hand, though virtually no TCRBV19-1- and TCRBV20-1-bearing cells were detected in the spleen, lymph nodes, and the thymus, they were apparently present in the intestinal tract and, to a lesser extent, in the lung.

Smaller numbers of subfamilies were detected with weak signals in the liver, seminal vesicles, uterus, bone marrow, and brain and their repertoires differed from those in the spleen, lymph nodes, and the thymus (data not shown).

Comparison of TCR repertoires in mice of different sexes and ages

The TCRBV repertoires were analyzed in the spleen, lymph nodes, and the thymus from 3- and 7-week-old male and female mice (12 groups). The TCRBV repertoires in mice of each sex and age are shown in Fig. 2. The percentages of TCRBV15-1-bearing cells were significantly higher in males than in females in both age groups, but there were no apparent differences in any of the other TCR repertoires. On the other hand, the percentage of TCRBV1-1-bearing cells was significantly decreased in the spleen, lymph nodes, and the thymus in 7-week-old mice compared with 3-week-old mice, whereas the percentages of TCRBV8-3- and 14-1-bearing cells were significantly increased in lymphatic organs of older mice.

Alterations in T cell populations in the thymus and spleen induced by HC administration (Table 2)

The number of thymic T cells decreased from 32.5 × 10^7 to 2.9 × 10^7 after HC administration, indicating the dose adopted in this study was effective. In control mice, approximately 80% of the thymic lymphocytes were

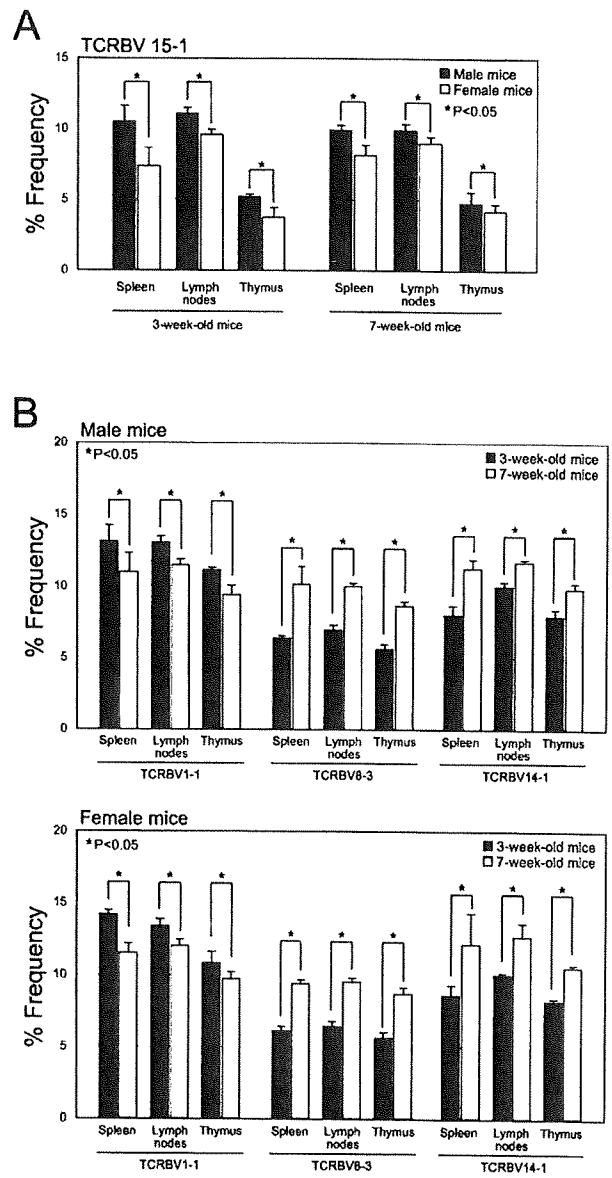

Fig. 2. Comparison of the TCR repertoires in mice of different sexes and ages. (A) Percentages of TCRBV15-1-bearing cells in the spleen, lymph nodes, and thymus of male (black bars) and female (white bars) mice at 3 weeks (left) and 7 weeks (right) of age. Vertical error bars indicate the standard deviation of five independent experiments. The TCR repertoires of these three organs were significantly higher in male mice than in female mice ($P<0.05$). (B) Percentages of TCRBV1-1-, 8-3-, and 14-1-bearing cells in the spleen, lymph nodes, and thymus of male (upper panel) and female (lower panel) mice at 3 weeks (black bars) and 7 weeks (white bars) of age. Vertical error bars indicate the standard deviation of five independent experiments. These three TCR repertoires differ significantly between the two ages ($P<0.05$).

Table 2. Changes in the percentages of CD4/CD8 T cell populations after administration of HC

	Number of CD3-positive cells ($\times 10^7$ cells)	Mean percentage of population ± SD			
		($CD4^+CD8^+$)	($CD4^+CD8^-$)	($CD4^-CD8^+$)	($CD4^-CD8^-$)
Thymus (PBS control)	32.5 ± 5.8	79.1 ± 0.7	10.6 ± 0.3	5.1 ± 0.5	5.2 ± 0.6
Thymus (HC)	2.9 ± 0.7[a)]	49.5 ± 9.6[b)]	26.1 ± 4.5[b)]	13.3 ± 2.2[b)]	11.0 ± 3.3[b)]
Spleen (PBS control)	21.1 ± 0.2	0.7 ± 0.1	67.4 ± 0.5	28.7 ± 0.6	3.3 ± 0.1
Spleen (HC)	14.4 ± 0.1[a)]	0.6 ± 0.1	67.6 ± 1.6	29.7 ± 1.2	2.1 ± 0.4

[a)]Number of CD3-positive cells differed significantly between PBS control and HC ($P<0.05$). [b)]CD4/CD8 population differed significantly between PBS control and HC in thymus ($P<0.05$).

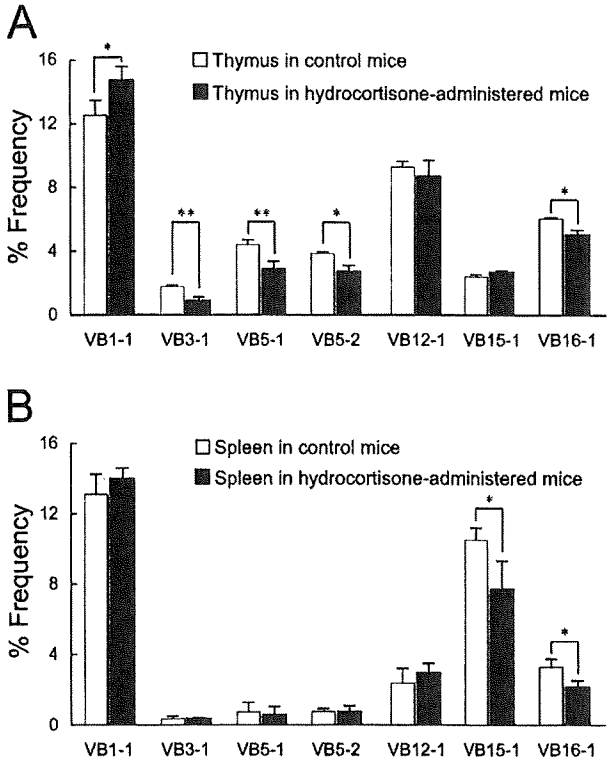

Fig. 3. Alterations in the TCR repertoires in the thymus and spleen after administration of HC. The percentages of cells bearing each TCRBV in control mice (white bars) and HC-administered mice (black bars) are shown. Panel (A) shows the TCRBV repertoires in the thymus. Panel (B) shows the TCRBV repertoires in the spleen. Vertical error bars indicate the standard deviation of five independent experiments. The families showing significant differences by Student's paired *t*-test are marked with asterisks (*$P<0.01$; **$P<0.005$).

$CD4^+CD8^+$ T cells, while $CD4^+CD8^-$ T cells and $CD4^-CD8^+$ T cells accounted for 11 and 5% of the cells, respectively. In contrast, in mice administered HC, $CD4^+CD8^+$ T cells, $CD4^+CD8^-$ T cells, and $CD4^-CD8^+$ T cells comprised 50, 26, and 13% of the thymic cells, respectively. The number of splenic T cells was decreased from 21.1×10^7 to 14.4×10^7 by HC. The CD4/CD8 T cell ratio, however, did not alter at all.

Alterations in TCR repertoire in the thymus and spleen induced by HC

The alterations observed in the TCR repertoire are shown in Fig. 3. The percentages of cells bearing TCRBV3-1, 5-1, 5-2, and 16-1 in the thymus significantly decreased in HC-treated mice compared with control mice. On the contrary, the percentage of cells bearing TCRBV1-1 in the thymus significantly increased in HC-treated mice. Cells bearing TCRBV15-1 and 16-1 in the spleen significantly decreased in HC-treated mice. The VB1-1 spleen T cells increased in number though not significantly.

Discussion

The thymus showed an unique TCRBV expression pattern among the organs examined in this study. Endogenous superantigens (SAGs) derived from mouse mammary tumor virus (MMTV) affect TCR repertoire by deleting T cells bearing particular VB chains either partially or completely in the thymus and peripheral lymphatic organs [2, 5, 21, 26]. BALB/c ($H\text{-}2^d$) mice express the Mtv-6, -8, and -9 genes from MMTV. The Mtv-6 SAG deletes $TCRBV3^+$ cells, while the Mtv-8 SAG deletes both $TCRBV11^+$ and 12^+ T cells [2, 21]. The Mtv-9 SAG induces clonal deletion of T cells bearing TCRBV5-1, 5-2, 11, and 12 [2, 21]. The expression patterns shown in the present study revealed that the percentages of virtually all these TCRBV subfamilies were low in peripheral lymphatic tissues, consistent with

the previous reports. TCRBV11$^+$ T cells, supposed to be deleted in BALB/c mice, however, were not deleted in the peripheral lymphatic tissues. We cannot think of an appropriate reason for this discrepancy. In addition, TCRBV16$^+$ T cells were incompletely deleted in the periphery, implying an alternative mechanism for the deletion of particular T cell clones other than SAGs.

The higher frequency of TCRBV15$^+$ T cells in lymph nodes and the spleen compared to the thymus suggest that another unknown peripheral positive selection or expansion mechanism is at work in the peripheral lymphatic organs.

Weak but detectable TCR signals were seen in the lung and intestinal tract. The lung, exposed to airborne foreign antigens through ventilation, possesses bronchus-associated lymphoid tissues (BALTs) [15]. Similarly, the intestinal tract, constantly exposed to food antigens and bacterial flora, has gut-associated lymphoid tissues (GALTs) [24]. Interestingly, in both the lung and the intestinal tract, although a TCR repertoire was observed that was generally consistent with that of the spleen and lymph nodes, TCRBV8-2$^+$ and 14$^+$ T cell numbers were decreased, whereas those of TCRBV19-1$^+$ and 20-1$^+$ T cells were increased. Since these organs have external milieu within and are exposed to external antigens, this condition might cause unique TCR repertoire changes (decrease of TCRBV8-2$^+$ and 14$^+$ T cells, and increase of TCRBV19-1$^+$ and 20-1$^+$ T cells). Unknown selection mechanisms may be functioning in the lung and in the intestinal tract. It was reported recently that an intestinal indigenous microbiota affect gene expression and cell activity of T cell, in a comparative study of SPF and germ free mice [9, 16]. The fact that the extent of expression of TCRBV19-1 and 20-1 in lymphocytes from the intestinal tract was greater than that from the lung may be due to the exposure to indigenous microbiota and/or food antigens. To address this issue, analyses with germ free animals would be gently helpful.

Sufficiently high signals for TCR analysis were not obtained for the liver, genital organs, the bone marrow and the brain. The relative CD3 mRNA expression levels were also low in these organs, suggesting that they contained only small T cell populations.

We further investigated whether the TCR repertoire would vary in normal mice according to sex and age. The frequency of TCRBV15-1-bearing cells was found to be higher in male than in female mice, irrespective of the age of the lymphatic tissues examined. The frequencies of TCRBV1-1-, 8-3-, and 14-1-bearing cells differed with age, with TCRBV8-3 and 14-1 higher showing in older mice.

The precise mechanisms behind these differences remain unknown. Various T cell selection systems, positive and/or negative, might be in operation systematically and/or locally, responding to genetic (sex) and/or environmental (tissue types and age) changes, leading to the alteration of the T cell repertoire. It is interesting, though, that indistinguishable age-dependent changes in the frequencies of TCRBV1-1-, 8-3-, and 14-1-bearing cells were found irrespective of the type of lymphatic tissue. In age-dependent changes, either an identical selection mechanism would operate in different lymphatic tissues including the thymus and lymph nodes, or similar genetic alterations would occur. Further extensive investigations of this are necessary.

HC-administered mice were found to have decreased numbers of CD4$^+$CD8$^+$ T cells in the thymus, suggesting that CD4$^+$CD8$^+$ T cells are HC-sensitive as previously reported [20]. The TCR repertoire in the thymus was also altered by HC treatment, as indicated by the decreased numbers of cells bearing TCRBV3-1, 5-1, 5-2, and 16-1. In peripheral T cells, MMTV sensitization causes clonal deletion of a proportion of the TCR families, including cells bearing TCRBV3-1, 5-1, 5-2, and 12-1 [2, 5, 21, 26]. In the present study, cells bearing TCRBV3-1, 5-1, and 5-2 in the thymus were found to be HC-sensitive. The numbers of these cells were greatly decreased, but they were not completely eliminated. In the spleen, however, these cell subsets were not significantly decreased by HC treatment. The reason for the increase in cells bearing TCRBV1-1 remains unknown, but a relative increase might have occurred due to a reduction in number of other TCRBV cells. On the other hand, one population, TCRBV12-1, partially deleted in the periphery after MMTV sensitization [2, 21], was found to be HC-resistant in this study. Cells bearing TCRBV16-1, which are unaffected by MMTV-sensitization, decreased in both the spleen and the thymus after HC administration. Therefore, TCRBV3-1, 5-1, and 5-2 are sensitive to both MMTV and HC, while TCRBV12-1

is sensitive only to MMTV and TCRBV16-1 is sensitive only to HC. We think that the sensitivity of TCR cells against MMTV or HC are totally disparate. Thus, HC, a potent endogenous stimulus, might create an entirely different environment within, leading to an alternative immune status of downregulating or overreacting to various antigens.

In the spleen, HC administration was found to decrease the number of T cells only slightly. Cells bearing TCRBV15-1 in the spleen, however, decreased significantly after HC administration. The counterpart subset in the thymus was not decreased by HC, suggesting TCRBV15-1 thymocytes are not identical to those in the spleen. The extent of deletion of some TCRBV families may be due to MMTV and/or other endogenous stimuli, like steroid hormones. In fact, completely deleted families were TCRBV3-1, 5-1, and 5-2, and partially deleted families were TCRBV12-1 and TCRBV16-1. It is possible that the difference of HC and/or MMTV sensibility in thymocytes influences the deletion level of peripheral T cells to suggesting the HC-resistant thymic lymphocyte is not equivalent to the medullary thymocyte, and that the HC-sensitive immature thymic lymphocyte is different among TCRBV families.

References

1. Alam, A., Lambert, N., Lule, J., Coppin, H., Mazieres, B., de Preval, C., and Cantagrel, A. 1996. Persistence of dominant T cell clones in synovial tissues during rheumatoid arthritis. *J. Immunol.* 156: 3480–3485.
2. Barnett, A., Mustafa, F., Wrona, T.J., Lozano, M., and Dudley, J.P. 1999. Expression of mouse mammary tumor virus superantigen mRNA in the thymus correlates with kinetics of self-reactive T-cell loss. *J. Virol.* 73: 6634–6645.
3. Blomgren, H. and Andersson, B. 1969. Evidence for a small pool of immunocompetent cells in the mouse thymus. *Exp. Cell. Res.* 57: 185–192.
4. Davis, M.M. 1990. T cell receptor gene diversity and selection. *Annu. Rev. Biochem.* 59: 475–496.
5. Dyson, P.J. and Elliott, J.I. 1999. Chronic deletion, escape from deletion and activation of mouse mammary tumor virus superantigen-reactive T cells in C57BL/10 mice. *Eur. J. Immunol.* 29: 1456–1466.
6. Fujii, Y., Kitaura, K., Nakamichi, K., Takasaki, T., Suzuki, R., and Kurane, I. 2008. Accumulation of T-cells with selected T-cell receptors in the brains of Japanese encephalitis virus-infected mice. *Jpn. J. Infect. Dis.* 61: 40–48.
7. Godfrey, D.I., Kennedy, J., Mombaerts, P., Tonegawa, S., and Zlotnik, A. 1994. Onset of TCR-beta gene rearrangement and role of TCR-beta expression during $CD3^-CD4^-CD8^-$ thymocyte differentiation. *J. Immunol.* 152: 4783–4792.
8. Godfrey, D.I., Kennedy, J., Suda, T., and Zlotnik, A. 1993. A developmental pathway involving four phenotypically and functionally distinct subsets of $CD3^-CD4^-CD8^-$ triple-negative adult mouse thymocytes defined by CD44 and CD25 expression. *J. Immunol.* 150: 4244–4252.
9. Ishikawa, H., Tanaka, K., Maeda, Y., Aiba, Y., Hata, A., Tsuji, N.M., Koga, Y., and Matsumoto, T. 2008. Effect of intestinal microbiota on the induction of regulatory $CD25^+$ $CD4^+$ T cells. *Clin. Exp. Immunol.* 153: 127–135.
10. Leckband, E. and Boyse, E.A. 1971. Immunocompetent cells among mouse thymocytes: a minor population. *Science* 172: 1258–1260.
11. Levine, M.A. and Claman, H.N. 1970. Bone marrow and spleen: dissociation of immunologic properties by cortisone. *Science* 167: 1515–1517.
12. Livak, F., Tourigny, M., Schatz, D.G., and Petrie, H.T. 1999. Characterization of TCR gene rearrangements during adult murine T cell development. *J. Immunol.* 162: 2575–2580.
13. Matsutani, T., Yoshioka, T., Tsuruta, Y., Iwagami, S., and Suzuki, R. 1997. Analysis of TCRAV and TCRBV repertoires in healthy individuals by microplate hybridization assay. *Hum. Immunol.* 56: 57–69.
14. Matsutani, T., Yoshioka, T., Tsuruta, Y., Iwagami, S., Toyosaki-Maeda, T., and Suzuki, R. 2000. Quantitative analysis of the usage of human T-cell receptor alpha and beta chain variable regions by reverse dot-blot hybridization. *Methods Mol. Biol.* 134: 81–101.
15. Moyron-Quiroz, J.E., Rangel-Moreno, J., Kusser, K., Hartson, L., Sprague, F., Goodrich, S., Woodland, D.L., Lund, F.E., and Randall, T.D. 2004. Role of inducible bronchus associated lymphoid tissue (iBALT) in respiratory immunity. *Nat. Med.* 10: 927–934.
16. Munakata, K., Yamamoto, M., Anjiki, N., Nishiyama, M., Imamura, S., Iizuka, S., Takashima, K., Ishige, A., Hioki, K., Ohnishi, Y., and Watanabe, K. 2008. Importance of the interferon-alpha system in murine large intestine indicated by microarray analysis of commensal bacteria-induced immunological changes. *BMC. Genomics* 9: 192–206.
17. Oksenberg, J.R., Panzara, M.A., Begovich, A.B., Mitchell, D., Erlich, H.A., Murray, R.S., Shimonkevitz, R., Sherritt, M., Rothbard, J., Bernard, C.C., and Steinman, L.W. 1993. Selection for T-cell receptor V beta-D beta-J beta gene rearrangements with specificity for a myelin basic protein peptide in brain lesions of multiple sclerosis. *Nature* 362: 68–70.
18. Penit, C., Lucas, B., and Vasseur, F. 1995. Cell expansion and growth arrest phases during the transition from precursor ($CD4^-8^-$) to immature ($CD4^+8^+$) thymocytes in normal and genetically modified mice. *J. Immunol.* 154: 5103–5113.
19. Raff, M. 1971. Evidence for subpopulation of mature lymphocytes within mouse thymus. *Nat. New. Biol.* 229: 182–184.
20. Reichert, R.A., Weissman, I.L., and Butcher, E.C. 1986. Dual immunofluorescence studies of cortisone-induced thymic involution: evidence for a major cortical component

to cortisone-resistant thymocytes. *J. Immunol.* 136: 3529–3534.

21. Scherer, M.T., Ignatowicz, L., Pullen, A., Kappler, J., and Marrack, P. 1995. The use of mammary tumor virus (Mtv)-negative and single-Mtv mice to evaluate the effects of endogenous viral superantigens on the T cell repertoire. *J. Exp. Med.* 182: 1493–1504.
22. Sensi, M. and Parmiani, G. 1995. Analysis of TCR usage in human tumors: a new tool for assessing tumor-specific immune responses. *Immunol. Today* 16: 588–595.
23. Shiobara, N., Suzuki, Y., Aoki, H., Gotoh, A., Fujii, Y., Hamada, Y., Suzuki, S., Fukui, N., Kurane, I., Itoh, T., and Suzuki, R. 2007. Bacterial superantigens and T cell receptor beta-chain-bearing T cells in the immunopathogenesis of ulcerative colitis. *Clin. Exp. Immunol.* 150: 13–21.
24. Spahn, T.W. and Kucharzik, T. 2004. Modulating the intestinal immune system: the role of lymphotoxin and GALT organs. *Gut* 53: 456–465.
25. Stordeur, P., Poulin, L.F., Craciun, L., Zhou, L., Schandené, L., de Lavareille, A., Goriely, S., and Goldman, M. 2002. Cytokine mRNA quantification by real-time PCR. *J. Immunol. Methods.* 262: 229.
26. Vacchio, M.S. and Hodes, R.J. 1989. Selective decreases in T cell receptor V beta expression. Decreased expression of specific V beta families is associated with expression of multiple MHC and non-MHC gene products. *J. Exp. Med.* 170: 1335–1346.
27. Vandevyver, C., Mertens, N., van den Elsen, P., Medaer, R., Raus, J., and Zhang, J. 1995. Clonal expansion of myelin basic protein-reactive T cells in patients with multiple sclerosis: restricted T cell receptor V gene rearrangements and CDR3 sequence. *Eur. J. Immunol.* 25: 958–968.
28. Yoshida, R., Yoshioka, T., Yamane, S., Matsutani, T., Toyosaki-Maeda, T., Tsuruta, Y., and Suzuki, R. 2000. A new method for quantitative analysis of the mouse T-cell receptor V region repertoires: comparison of repertoires among strains. *Immunogenetics* 52: 35–45.

Clinical & Experimental Immunology
The Journal of Translational Immunology

Clinical and Experimental Immunology ORIGINAL ARTICLE doi:10.1111/j.1365-2249.2008.03763.x

Skew in T cell receptor usage with polyclonal expansion in lesions of oral lichen planus without hepatitis C virus infection

A. Gotoh,*† Y. Hamada,* N. Shiobara,† K. Kumagai,*† K. Seto,* T. Horikawa‡ and R. Suzuki†

*First Department of Oral and Maxillofacial Surgery, School of Dental Medicine, Tsurumi University, Yokohama, †Department of Rheumatology and Clinical Immunology, Clinical Research Center for Allergy and Rheumatology, National Sagamihara Hospital, Sagamihara, and ‡Division of Dermatology, Department of Clinical Molecular Medicine, Kobe University Graduate School of Medicine, Kobe, Japan

Accepted for publication 25 July 2008
Correspondence: R. Suzuki, Department of Rheumatology and Clinical Immunology, Clinical Research Center for Allergy and Rheumatology, National Sagamihara Hospital, 18-1 Sakuradai, Sagamihara, Kanagawa 228-0815, Japan.
E-mail: r-suzuki@sagamihara-hosp.gr.jp

Summary

Oral lichen planus (OLP) is a refractory disorder of the oral mucosa. Its predominant symptoms are pain and haphalgesia that impair the quality of life of patients. OLP develops via a T cell-mediated immune process. Here, we examined the characteristics of the infiltrating T cells in terms of the T cell receptor (TCR) repertoires, T cell clonality, T cell phenotypes and cytokine production profiles. TCR repertoire analyses and CDR3 size spectratyping were performed using peripheral blood mononuclear cells (PBMCs) and tissue specimens of OLP biopsies from 12 patients. The cytokine expression profiles and T cell phenotypes were measured by real-time quantitative polymerase chain reaction. We observed that there were skewed TCR repertoires in the tissue samples (TCRVA8-1, VA22-1, VB2-1, VB3-1 and VB5-1) and PBMCs (TCRVA8-1, VB2-1, VB3-1 and VB5-1) from OLP patients. Furthermore, the CDR3 distributions in the skewed TCR subfamilies exhibited polyclonal patterns. We observed increases in $CD4^+$ T lymphocytes, interleukin (IL)-5, tumour necrosis factor (TNF)-α and human leucocyte antigen D-related in the OLP tissue specimens. Taken together, the present results suggest that T cells bearing these TCRs are involved in the pathogenesis of OLP, and that IL-5 and TNF-α may participate in its inflammatory process.

Keywords: oral lichen planus, oral mucosa, superantigens, T lymphocytes, TCR repertoire

Introduction

Oral lichen planus (OLP) is a chronic inflammatory disease of the oral mucosa. Although the cause of OLP remains unclear, it is believed that certain patients with hepatitis C virus (HCV) infection and contact allergies to dental filling materials are susceptible to OLP [1]. Histopathologically, OLP is characterized by the presence of intraepithelial lymphocyte exocytosis, subepithelial band-like inflammatory infiltrates and hydropic degeneration of basal cells with apoptosis [2]. The infiltrating lymphocytes are composed predominantly of T cells with $CD4^+$ and $CD8^+$ phenotypes that express αβ T cell receptors (TCRs) [3]. $CD8^+$ T cells are found frequently adjacent to degenerated keratinocytes. Previously, several different TCR repertoires in lesions and peripheral blood mononuclear cells (PBMCs) of OLP patients have been reported, namely Vα2 and Vβ3 [4], Vβ13, Vβ14 and Vβ15 [5], Vβ2, Vβ16 and Vβ19 [6], and Vβ22 and Vβ23 [7]. Thus, the specific TCR repertoires in OLP lesions remain unclear.

T cells bearing TCRs recognize antigens in the form of peptide fragments in association with major histocompatibility complex (MHC) class I and class II molecules on antigen-presenting cells [8]. The fine specificity of T cells is determined by the TCRs displayed on the cell surface, which comprise heterodimers of an α-chain and a β-chain or a γ-chain and a δ-chain. The variable regions of these chains are responsible for antigen recognition and encoded by variable (V), joining (J) and diversity (D) gene segments. We have developed previously an adaptor ligation-mediated polymerase chain reaction (AL–PCR) method that allows us to define TCR repertoires based on the expression levels of transcripts, even when only small numbers of cells are available. This method enables us to amplify all the variable regions of the rearranged TCR genes through PCR cycles without skewing. Applying this method to a microplate hybridization assay (MHA) is simpler and more reproducible, and enables us to analyse TCR repertoires rapidly [9].

Random insertion of non-germinal element (N) nucleotides or deletion of nucleotides has been observed in the VN (D) NJ junction region designated CDR3, and is thought to be responsible for the antigenic peptide content [10,11]. Thus, any specific recognition of antigens by CDR3 can lead

